ANP-2843Q1NP
Revision 0

LaSalle Unit 2 Nuclear Power Station Spent Fuel Storage Pool Criticality Safety Analysis with Neutron Absorbing Inserts and Without Boraflex - RAIs

June 2010

AREVA NP Inc.

AREVA

LaSalle Unit 2 Nuclear Power Station Spent Fuel Storage Pool Criticality Safety Analysis with Neutron Absorbing Inserts and Without Boraflex - RAIs

Copyright © 2010

AREVA NP Inc.

All Rights Reserved

Abstract

Responses to thirty-five (35) of the forty-five (45) RAIs (Reference 1) with regard to the LaSalle Unit 2 Nuclear Power Station Spent Fuel Storage Pool Criticality Safety Analysis with Neutron Absorbing Inserts and Without Boraflex are provided by this document. The ten (10) RAIs not contained within this document are RAIs 3, 4, 6, 7, 13, 15, 29, 30, 31, and 33.

The response to an additional RAI (Reference 4) received later is also included in this report.

Nature of Changes

Item	Page	Description and Justification
1.	All	This is a new document.

Contents

1. Introduction 1

2. Responses to Request for Additional Information 2
   2.1 Request for Additional Information No. 1 2
   2.2 Request for Additional Information No. 2 4
   2.3 Request for Additional Information No. 5 6
   2.4 Request for Additional Information No. 8 7
   2.5 Request for Additional Information No. 9 11
   2.6 Request for Additional Information No. 10 12
   2.7 Request for Additional Information No. 11 13
   2.8 Request for Additional Information No. 12 18
   2.9 Request for Additional Information No. 14 19
   2.10 Request for Additional Information No. 16 20
   2.11 Request for Additional Information No. 17 21
   2.12 Request for Additional Information No. 18 23
   2.13 Request for Additional Information No. 19 24
   2.14 Request for Additional Information No. 20 27
   2.15 Request for Additional Information No. 21 28
   2.16 Request for Additional Information No. 22 31
   2.17 Request for Additional Information No. 23 36
   2.18 Request for Additional Information No. 24 38
   2.19 Request for Additional Information No. 25 43
   2.20 Request for Additional Information No. 26 44
   2.21 Request for Additional Information No. 27 45
   2.22 Request for Additional Information No. 28 46
   2.23 Request for Additional Information No. 32 56
   2.24 Request for Additional Information No. 34 57
   2.25 Request for Additional Information No. 35 61
   2.26 Request for Additional Information No. 36 62
   2.27 Request for Additional Information No. 37 65
   2.28 Request for Additional Information No. 38 71
   2.29 Request for Additional Information No. 39 72
   2.30 Request for Additional Information No. 40 75
   2.31 Request for Additional Information No. 41 79
   2.32 Request for Additional Information No. 42 82
   2.33 Request for Additional Information No. 43 83
   2.34 Request for Additional Information No. 44 84
   2.35 Request for Additional Information No. 45 85

3. Follow-up Request for Additional Information 88

4. References 90

This document contains a total of 98 pages.

Tables

Table RAI-8.1: In-Rack k_∞ Sensitivity to In-core Depletion Temperature 8
Table RAI-8.2: In-Rack k_∞ Sensitivity to In-core Depletion Power Density 9
Table RAI-8.3: Effect of Neglecting Aluminum, Boron-11 and Carbon in the Insert on In-Rack k_∞ 10
Table RAI-10.1: Impact of Channel Thickness on In-Rack Reactivity 12
Table RAI-17.1: Channel Cross-Sectional Area 21
Table RAI-22.1: Reactivity Decrement for Bounding Lattices 33
Table RAI-22.2: Reactivity Decrement for Limiting ATRIUM-10 Lattices 33
Table RAI-25.1: Limiting ATRIUM-9 to Bounding Lattice Comparison (in-rack) 43
Table RAI-28.1: 8X8 Lattice Screening based upon Cold In-core Geometry 50
Table RAI-28.2: Maximum in-Rack k_∞ For 8x8 Fuel 51
Table RAI-28.3: ATRIUM-9B Lattice Screening based upon Cold In-core Geometry 52
Table RAI-28.4: Maximum in-Rack k_∞ For ATRIUM-9B Fuel 52
Table RAI-28.5: GE14 Lattice Screening based upon Cold In-Core Geometry 53
Table RAI-28.6: Maximum in-Rack k_∞ For GE14 Fuel 53
Table RAI-28.7: ATRIUM-10 Lattice Screening based upon Cold In-Core Geometry 54
Table RAI-34.1: Manufacturing Reactivity Uncertainties 60
Table RAI-37.1: LaSalle Fuel Product Lines Used 68
Table RAI-37.2: Uncontrolled and Controlled Depletion 68
Table RAI-37.3: LaSalle Failed Fuel Assemblies 69
Table RAI-39.1: Comparison of Parameters for Datasets with and without MOX 73
Table RAI-45.1: CASMO-4 to KENO Lattice Geometry Dependence at 4°C 86
Table RAI-U.1: KENO Axial Boundary Condition Comparisons 89

Figures

Figure RAI-11.1: Most Reactive Bottom Lattices (0" to 96") 15
Figure RAI-11.2: Most Reactive Intermediate Lattices (96" to 126") 16
Figure RAI-11.3: Most Reactive Top Lattices (above 126") 17
Figure RAI-19.1: Combined Assembly Rotation Scenarios 25
Figure RAI-21.1: Impact of Void History Depletion on In-Rack k_∞ 30
Figure RAI-22.1: Depletion Penalty Assessment 34
Figure RAI-22.2: LaSalle Unit 2 Storage Pool In-Rack k_∞ Comparison 35
Figure RAI-24.1: LaSalle Unit 2 Spent Fuel Pool 41
Figure RAI-24.2: Limiting Missing Insert Condition 42
Figure RAI-35.1: Overview of the ANP-2843(P) Criticality Safety Analysis 61
Figure RAI-39.1: Evaluation for Pu Trend 74
Figure RAI-40.1: Evaluation for EALF Trend 78
Figure RAI-40.2: Evaluation for Enrichment Trend 78

1. Introduction

This document provides responses to requests for additional information (RAI) from the Nuclear Regulatory Commission (References 1 and 4) in regard to a license amendment request submitted by Exelon Nuclear (Reference 2). The subject license amendment request supports the installation of neutron absorbing inserts into the LaSalle Unit 2 Spent Fuel Pool (SFP) storage racks. This document addresses the RAIs involving the criticality safety analysis (Reference 3) which was included as Attachment 3 of the Reference 2 license amendment request. Specifically, this document contains responses to RAIs 1 through 45 of Reference 1 with the exception of RAIs 3, 4, 6, 7, 13, 15, 29, 30, 31, and 33. The responses to the excepted RAIs will be provided by Exelon outside of this report. This report also includes the response to an RAI provided in Reference 4.

2. Responses to Request for Additional Information

This section provides the responses to thirty-five of the USNRC requests for additional information provided in Reference 1.

2.1 *Request for Additional Information No. 1*

Text from Attachment 1, "Evaluation of Proposed Change," Section 3.2, "Criticality," Page 10, 2nd paragraph after the bulleted list:

> *As the rack inserts are installed, there will be interface conditions between spent fuel storage racks with credit for Boraflex and no credit for the NETCO-SNAP-IN® rack inserts, and spent fuel storage racks with no credit for Boraflex and credit for NETCO-SNAP-IN® rack inserts. The reactivity state of the two storage configurations both meet the 0.95 K_{eff} storage criteria and therefore, by definition, both configurations are acceptable for storage in the LSCS Unit 2 SFP.*

It is not clear that this statement is true. The criticality safety analyses for the NETCO insert and Boraflex regions likely have different fuel assembly acceptance criteria. Thus, an assembly might be acceptable for storage in one region and not the other. Further, due to the location of the inserts in the NETCO insert racks, the interface between Boraflex and NETCO insert rack modules may require further evaluation or additional controls, such as the commitment stated in the criticality safety analysis to install inserts in neighboring Boraflex racks.

Provide clarification or additional justification for this statement.

Response:

The impact of the change on the current criticality safety analyses is best described by examining the impact on the boundary conditions assumed in these analyses. As noted above, a regulatory commitment has been made to install inserts into the cells of an otherwise unmodified Boraflex rack that is adjacent to a rack with NETCO-SNAP-IN® inserts. This establishes a "buffer zone" that contains a combination of neutron poison from both the Boraflex rack and from the NETCO-SNAP-IN® insert. This "buffer zone" consequently represents an area of lower reactivity than was assumed in the original analyses.

As noted by the reviewer in RAI-2, the NETCO-SNAP-IN® insert criticality safety analysis in ANP-2843(P) assumes the use of lower reactivity assemblies than was assumed for the current Boraflex analysis. The ANP-2483(P) analysis has also confirmed that all existing fuel meets the lower reactivity requirements of the NETCO-SNAP-IN® insert criticality safety analysis (this is addressed further in the responses to RAI-28 and RAI-37). Furthermore, the Technical Specifications change ensures that all future ATRIUM-10 fuel for LaSalle will continue to meet this lower allowable reactivity requirement.

- The combination of these controls, regulatory commitment and Technical Specifications change, assures that the buffer zone provides a boundary between the racks that is of a lower reactivity than the boundary condition assumed in the original analyses.
- The additional poison material (combination of both the Boraflex and the NETCO-SNAP-IN® insert) is conservative to both analyses, and
- The allowable reactivity bundle definition meets the new NETCO-SNAP-IN® insert criticality safety analysis requirements and is of a lower reactivity than supported by the current Boraflex criticality safety analysis.

Therefore, bundles meeting the new Technical Specifications requirement, which will apply to both the BORAFLEX region and NETCO Insert region of the spent fuel pool, will meet the storage requirements for both the current Boraflex and new NETCO-SNAP-IN® insert criticality analyses.

The regulatory commitment to install the inserts in adjacent rack cells is documented in Attachment 7 of the LAR. The controls regarding the interface of Boraflex and NETCO-SNAP-IN® insert racks is addressed in the response to RAI-33.

2.2 *Request for Additional Information No. 2*

Text from Attachment 1, Section 3.2, Page 10, 5th paragraph after the bulleted list:

> *Finally, the criticality analysis provided in Attachment 3 has employed a less reactive fuel assembly than that used in the most recent LSCS Unit 1 BORAL® SFP criticality analysis, and the most recent LSCS Unit 2 Boraflex SFP criticality analysis. The proposed change also includes a revision to TS Section 4.3.1 to specify this less reactive fuel as the most reactive assembly allowed for storage in either the Unit 1 or Unit 2 SFPs.*

The potential impact on either the LSCS Unit 1 BORAL or LSCS Unit 2 Boraflex criticality analyses by the installation and use of the NETCO-SNAP-In® rack inserts in LSCS Unit 2 has not been evaluated in the AREVA SFP criticality analysis (ANP-2843P, proprietary). Such an evaluation should be performed and documented.

Response:

This RAI requests an evaluation of the impact of the change to the existing Unit 1 and Unit 2 criticality analyses. The requested Technical Specifications change for the detailed storage requirements limits the allowable reactivity for storage in both SFPs to the least reactive assembly supported by the different criticality analyses. This change is necessary to allow transfer of assemblies between SFPs while ensuring that the criticality requirements for each pool are met. The impact on the various SFP analyses is discussed in more detail for each unit below:

Unit 1: As noted in the RAI the NETCO-SNAP-IN® inserts will only be installed in the Unit 2 spent fuel pool. Therefore, the installation of inserts into the Unit 2 SFP has no direct impact on the existing Unit 1 BORAL criticality analysis since the pools are physically separated and therefore neutronically isolated. However, the Unit 1 and 2 SFPs are connected by a transfer canal and the potential exists that bundles may be moved between pools. Since the new NETCO-SNAP-IN® insert criticality analysis assumes a less reactive assembly than the Unit 1 Boral analysis, a change is being requested to TS section 4.3.1 to limit storage in both pools to assemblies meeting this lower reactivity requirement. All bundles currently stored in the Unit 1 SFP (and the Unit 2 SFP) already meet this lower reactivity requirement as shown in Appendix B and discussed in the responses to RAI-28 and RAI-37. The TS Section 4.3.1

change will ensure that future bundles continue to meet this requirement. No change is required to the existing Unit 1 BORAL criticality analysis since it is always acceptable to load a lower reactivity assembly than supported by the analysis. In other words, the requested Technical Specifications change lowering the allowable reactivity of the assembly that can be stored in the pool is conservative in regard to the existing Unit 1 criticality analysis.

Unit 2: The NETCO inserts will be installed in the Unit 2 SFP in large regions (i.e. by racks) as the inserts become available. In this transition period, the Unit 2 SFP will contain a mixture of Boraflex racks and racks containing the NETCO inserts. The intent is that the existing criticality analysis will continue to support the unmodified racks as well as those storage locations between the regions that credit Boraflex and also contain an insert. Those regions that contain inserts and do not credit Boraflex will be supported by ANP-2843(P). Upon completion of the modification (i.e. all accessible locations contain NETCO-SNAP-IN® inserts) ANP-2843(P) will supersede the existing Boraflex criticality analysis. The change to TS 4.3.1 to use a lower reactivity assembly than supported by the current Unit 2 SFP Boraflex analysis represents a conservative change since it is always acceptable to load a lower reactivity assembly than supported by the analysis. In other words, the requested Technical Specifications change lowering the allowable reactivity of the assembly that can be stored in the pool is conservative in regard to the existing Unit 2 Boraflex criticality analysis. Transition impacts are addressed in the response to RAI-1.

Conclusion: The requested change to TS section 4.3.1 represents an increase in conservatism for the current analyses for each SFP since it reduces the allowable reactivity of an assembly. Transition impacts on the Unit 2 SFP are conservatively controlled by a regulatory commitment to install the NETCO-SNAP-IN® inserts into the cells adjacent to racks containing the inserts as discussed in the response to RAI-1 and RAI-33.

2.3 *Request for Additional Information No. 5*

Text from Attachment 1, Section 3.8.3, "Fuel Assembly Place Alongside Spent Fuel Storage Rack," describes an assembly placed outside the racks. From the description, it is not clear that the most reactive configuration was considered.

Confirm that an assembly placed into an interior corner of three rack modules, with outer walls not covered by inserts (see figure), was evaluated. The analysis should also look at variations in spacing between the external assembly, with and without fuel channel, and the storage rack modules.

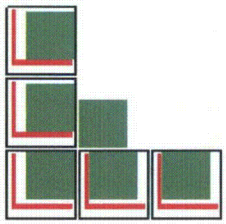

Response:

This configuration was evaluated and was determined to be bounded by the missing insert condition. This evaluation is discussed in detail in the response to RAI-24.

2.4 *Request for Additional Information No. 8*

Report ANP-2843(P) (proprietary), Section 2.0, 5th paragraph provides guidance for evaluating the reactivity of lattices for comparison with the limiting rack infinite multiplication factor (k_∞) values. The reader is referred to the CASMO-4 models provided in Appendix A. Considering the nature of how these models will be used, the NRC staff will need to review them.

Provide the CASMO-4 manual for use in the review. These input files inherently rely on several approximations and assumptions related to in-core depletion and in-rack k_∞ calculations.

Consistent with the guidance provided in Standard Review Plan 9.1.1. "New Fuel Storage," identify and justify approximations and assumptions used. Where appropriate, quantify biases and uncertainties associated with approximations and assumptions used.

Response:

A copy of the CASMO-4 user's manual will be provided to the NRC in accordance with the license agreement between AREVA and Studsvik/Scandpower for the NRC to complete their assessment. The CASMO-4 Users Manual is proprietary to Studsvik/Scandpower and should be treated accordingly.

Modeling Assumptions:

The application of CASMO-4 for in-core fuel depletion is consistent with the NRC approval of EMF-2158(P)(A). Input for the depletion calculation includes the fuel assembly material and geometry.

<u>Assumption 1</u>: The top of the part length rods in the ATRIUM-10 assembly, which contain a 6 inch plenum, can be treated as a water hole in the lattice in-core depletion and in the in-rack calculations. The actual content of the 6 inch plenum consists of a stainless steel spring and fill gas. Neglecting the 6 inch plenum is conservative from a criticality stand point because it results in a more reactive condition than would exist with the exclusion of the moderator and the neutron absorption of the plenum spring material.

Assumption 2: A fuel temperature is assumed for the fuel depletion based on the core average linear heat generation rate. Consistent fuel temperatures are used for a given geometry. Sensitivity studies were performed to determine the impact of the fuel temperature used in the fuel depletion on the in-rack storage reactivity. The fuel temperature was varied plus and minus 100 °F relative to the base depletion temperature for the reference bounding lattices.

The highest temperature produced the most reactive in-rack k_∞. For an increase of 100 °F, the largest increase in the in-rack k_∞ was 0.00014 Δk. Table RAI-8.1 provides the in-rack results based on in-core depletion at the different temperatures (i.e. the cold in-rack calculations were repeated for the in-core depletions performed at the different temperatures). The small change in reactivity with respect to the in-core depletion temperature does not impact the ability to select the most reactive lattice for the actual criticality evaluations performed with KENO.

Table RAI-8.1: In-Rack k_∞ Sensitivity to In-core Depletion Temperature

	k_∞ versus Temperature		
Bottom Geometry	**865.6 °F**	**965.5 °F**	**1065.4 °F**
A10B-4570L-10G60_BL	0.88421	0.88434	0.88448
Top Geometry	**906.4 °F**	**1006.3 °F**	**1106.2 °F**
A10T-4470L-10G35_BL	0.91848	0.91858	0.91867
A10T-4570L-10G60_BL	0.88679	0.88691	0.88702

Assumption 3: The moderator temperature used for in-core depletion is assumed to be at saturated conditions corresponding to the rated pressure. The more important parameter in a BWR reactor is the actual moderator density/void level. Three explicit void conditions are used to perform the in-core depletion calculations. (Additional information and justification for the void levels is provided in response to RAI-21.)

Assumption 4: The power density used for the fuel depletion is based on the core rated power per unit volume. Table RAI-8.2 provides the reactivity effect as a function of power density. 100% power density represents the core average power density at rated power. This sensitivity analysis was performed for the limiting gadolinia lattices in Table B.2 of ANP-2843(P). These results show that the power density assumed during fuel depletion has minimal impact on the

in-rack results. Furthermore, depletion at the core average power density is consistent with AREVA's standard NRC-approved depletion methodology. This procedure is therefore consistent with the uncertainties defined in EMF-2158(P)(A) as described in Appendix D of ANP-2843(P) and the response to RAI-41.

Table RAI-8.2: In-Rack k_∞ Sensitivity to In-core Depletion Power Density

	Uncontrolled		
	150% PD	**100% PD**	**50% PD**
Bottom			
A10B-4399L-12G65	0.870	0.871	0.872
A10B-4510L-13G75	0.863	0.863	0.865
A10B-4537L-13GV70	0.856	0.857	0.859
A10B-4538L-13GV80	0.844	0.844	0.846
Intermediate			
A10T-4313L-15G65	0.859	0.860	0.862
A10T-4524L-13GV70	0.859	0.860	0.861
A10T-4511L-15GV80	0.839	0.840	0.841
Top			
A10T-3947L-13GV38	0.882	0.882	0.884
A10T-4400L-10G45	0.906	0.907	0.908
A10T-4409L-10G45	0.906	0.907	0.908
A10T-4444L-12G40	0.907	0.907	0.909
ATRIUM-9			
A9-458L8G6	0.883	0.884	0.886

Assumption 5: Modeling of the pellet deformation with respect to burnup can be ignored for the in-core depletion and in-rack calculations. Modeling of the pellet deformation does not significantly change the neutronic characteristics of the fuel since the material content is unchanged.

Assumption 6: The spacer (i.e. spacer grid) material can be ignored in the in-core depletion and in-rack calculations. The spacer will exclude water and absorb neutrons. It will also have a minimal impact on the neutron spectrum. Ignoring the spacer material is conservative for BWR criticality analyses in that a slightly more reactive configuration is modeled.

Assumption 7: For the fuel storage rack model, the insert is assumed to have a 90° bend in the center and a full six inch wing length (see response to RAI-18 for more details). In addition the Aluminum, Boron-11, and Carbon are neglected. Both of these are conservative assumptions.

To confirm that this is conservative, CASMO-4 calculations were performed for the three REBOL lattices to specifically model the impact of adding these materials. The calculations resulted in lower k_∞ values than the calculations in which they were not included as shown in Table RAI-8.3.

Table RAI-8.3: Effect of Neglecting Aluminum, Boron-11 and Carbon in the Insert on In-Rack k_∞

Lattice	Base In-Rack K_∞[1] (Without AL,B11,C)	In-Rack K_∞ (Including AL,B11,C)
A10B-266L-0G0	0.89468	0.89427
A10T-272L-0G0	0.89774	0.89734
A10T-305L-0G0	0.92866	0.92826

Assumption 8: Within the fuel storage configuration, the stainless steel channel (i.e. fuel storage can) and the ½ water gap (the region where the Boraflex is assumed to have been replaced by water) are combined into a single mixture. This is required by a limitation of the CASMO-4 code system. The water density in this model is set to 1 gm/cm^3.

This modeling approximation does not adversely impact the ability of CASMO-4 to be used for the selection of lattices to be used by KENO in the criticality evaluation. Appendix D of ANP-2843(P) compares KENO (explicit modeling) and CASMO-4 with the fuel storage model simplification k_∞ results and shows good agreement between the two systems.

The impact of this modeling simplification was evaluated with KENO.[2] The KENO k_∞ value decreased by 0.002 Δk for the base configuration with this simplification. (The bias between the two code systems decreases with the inclusion of the CASMO model simplification into the KENO model.)

---

1 The report Base In-Rack k-infinity values are the same as those in Table B.1 of ANP-2843(P) except that they are reported here to 5 significant digits.

2 The KENO criticality geometry used for establishing compliance with the 0.95 keff limit explicitly models the stainless steel storage can and ½ water gap (the region where Boraflex is assumed to have been replaced) as physically unique separate regions.

2.5 *Request for Additional Information No. 9*

In ANP-2843(P) (proprietary), Section 2.0, the 3rd bulleted item includes the parenthetical phrase "no credit is taken for assembly burnup." This is incorrect and misleading. For assemblies with gadolinium (Gd), the peak-reactivity point takes credit for both fuel burnup and residual Gd. Uncertainties related to burnup-dependent fuel and Gd concentrations and reactivity worths should be applied to Gd lattices when they are compared to the bounding beginning of life (BOL) lattices.

Describe how such uncertainties are included in the analysis or justify not including these uncertainties.

Response:

The intent of the statement 'no credit is taken for assembly burnup' is to specify that this criticality safety analysis does not take credit for lower reactivity conditions associated with higher burnup fuel (i.e. as done in some PWR SFP criticality analyses). This analysis evaluates all lattices at peak reactivity conditions which represents a significant conservatism since it is not possible for all lattices in an assembly and thus all lattices in the SFP to reach this condition at the same time. Calculation uncertainties with respect to fuel burnup and gadolinia depletion are included in the analysis with the use of the 0.010 Δk adder between the bounding lattice designs and the REBOL lattice designs. This uncertainty is discussed within Section 5 and Appendix D of ANP-2843(P). The response to RAI-22 contains additional justification for the value applied.

2.6 *Request for Additional Information No. 10*

*ANP-2843(P) (proprietary), footnote * states that 80 mil fuel channels are acceptable. The analysis should show this to be the case by presenting results for both the 80 and 100 mil fuel channels.*

Confirm that calculations were performed for both 80 and 100 mil channels.

Response:

The calculation results for the 100 mil fuel channel, the 80 mil fuel channel, and without a channel are:

Table RAI-10.1: Impact of Channel Thickness on In-Rack Reactivity

Fuel Channel Thickness (mil)	(inch)	ANP-2843(P) Value (Rounded up)	KENO V.a k_∞ Result
100	0.100	0.916	0.9152
80	0.080	---	0.9131
0	0	~0.910 [1]	0.9092

Therefore, the 100 mil channel bounds the results for an 80 mil channel since in-rack reactivity decreases with decreasing channel thickness. Similarly, assuming the use of a 100 mil channel is bounding for unchanneled fuel.

[1] This is identified as *"... about 0.006 Δk lower when fuel channels are removed"* in Section 6.3 of ANP-2843(P). The actual calculated value is provided in the adjacent column.

2.7 *Request for Additional Information No. 11*

ANP-2843(P) (proprietary), Section 2.0, bullet item on page 2-3. This claim is not substantiated. The uncertainties in keff will vary with things like assembly design, initial ^{235}U enrichment, burnup-dependent fuel and Gd compositions, initial Gd content, number of Gd rods, fuel enrichment, part-length versus full length rod lattices, etc.

Strengthen the analysis supporting this claim.

Response:

The uncertainties in k_{eff} vary with:

1) manufacturing tolerances,
2) fuel design flexibility, and
3) modeling (codes and libraries) uncertainty.

The uncertainties due to manufacturing tolerances are applied in the $k_{95/95}$ determination through the Δk_{tol} term (ANP-2843(P) page 6-6). Additional discussion on the treatment of uncertainty due to manufacturing tolerances is provided in the response to RAI-34.

The acceptance criteria presented within the document apply to future ATRIUM-10 assemblies (as discussed in the response to RAI-12). All existing assembly designs in the LaSalle Unit 1 and Unit 2 SFP have been evaluated and the results for the limiting lattices are provided in Appendix B of ANP-2843(P) (as discussed in the responses to RAI-28 and RAI-37). Therefore design flexibility is only considered for ATRIUM-10 fuel.

The approach used in the analysis is to bound fuel design flexibility with a bounding lattice design. This allows design freedom while not challenging uncertainties associated with the criticality safety analysis.

As noted above, design flexibility applies to future ATRIUM-10 assemblies since all current designs have been evaluated. The approach used in determining the bounding ATRIUM-10 lattice designs is illustrated in Figures RAI-11.1 through RAI-11.3. These figures graphically show the reactivity of each of the limiting lattices identified in Appendix B for the bottom,

intermediate and top elevation zones, respectively, of the ATRIUM-10 design. The corresponding bounding lattice and REBOL reactivities are also provided for comparison. (Note: The data in Figures RAI-11.1 through RAI-11.3 is plotted using four significant digits. This is consistent with the response to RAI-22 and not the three significant digits provided in Appendix B of ANP-2843(P).)

The 0.010 Δk addresses CASMO-4 bias and uncertainties with respect to fuel burnup. (See response to RAI-22 and RAI-35) KENO bias and bias uncertainty are included in the $k_{95/95}$ formulation.

The adequacy of the 0.010 Δk adder applied in the development of the REBOL from the bounding lattice is discussed in Appendix D of ANP-2843(P). An alternate method of supporting the magnitude of this adder is provided in the response to RAI-22 in which burnup dependent (Δkbu) and residual gadolinia (Δkgd) reactivity corrections are introduced. Figures RAI-11.1 through RAI-11.3 provide the adjusted k_∞ that includes these adders (i.e. $k_{adj}=k_\infty+\Delta kbu+\Delta kgd$). This shows that in all cases the REBOL reactivity bounds both existing lattices and the reference bounding lattices, thus confirming the adequacy of the 0.010 Δk adder.

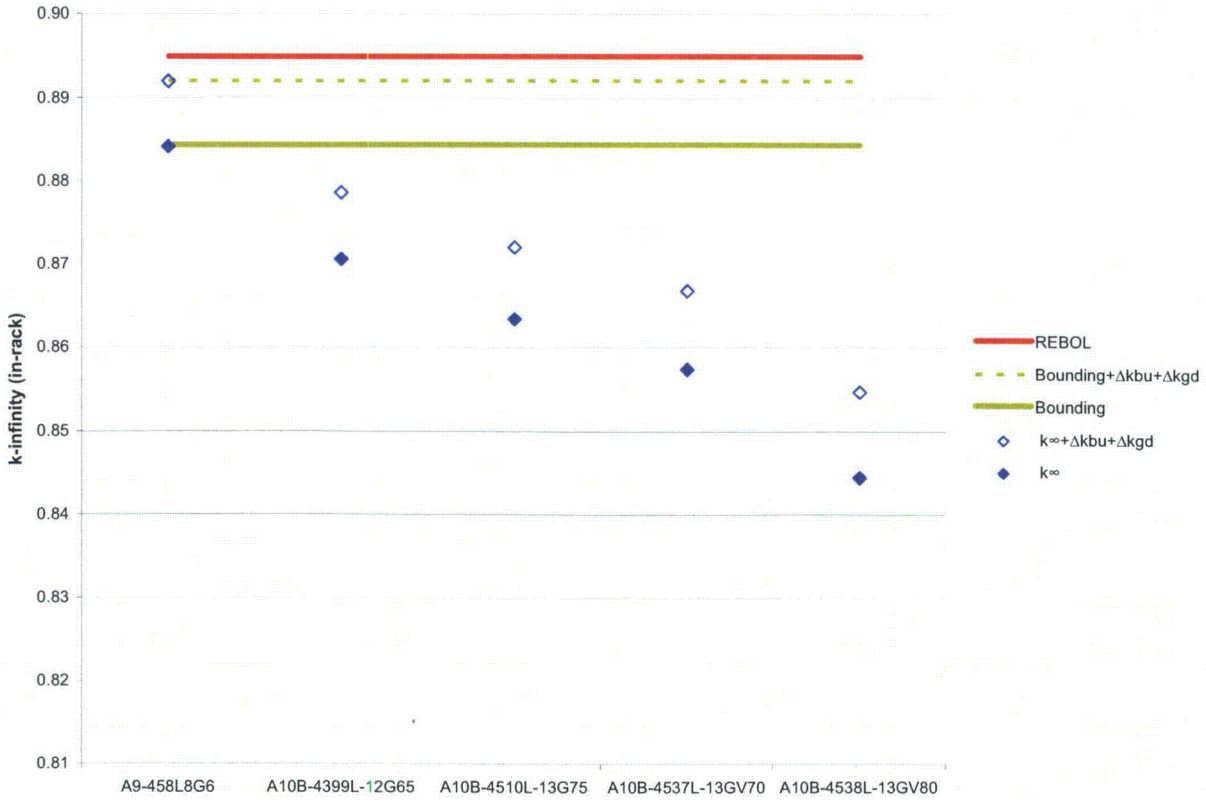

Figure RAI-11.1: Most Reactive Bottom Lattices (0" to 96")

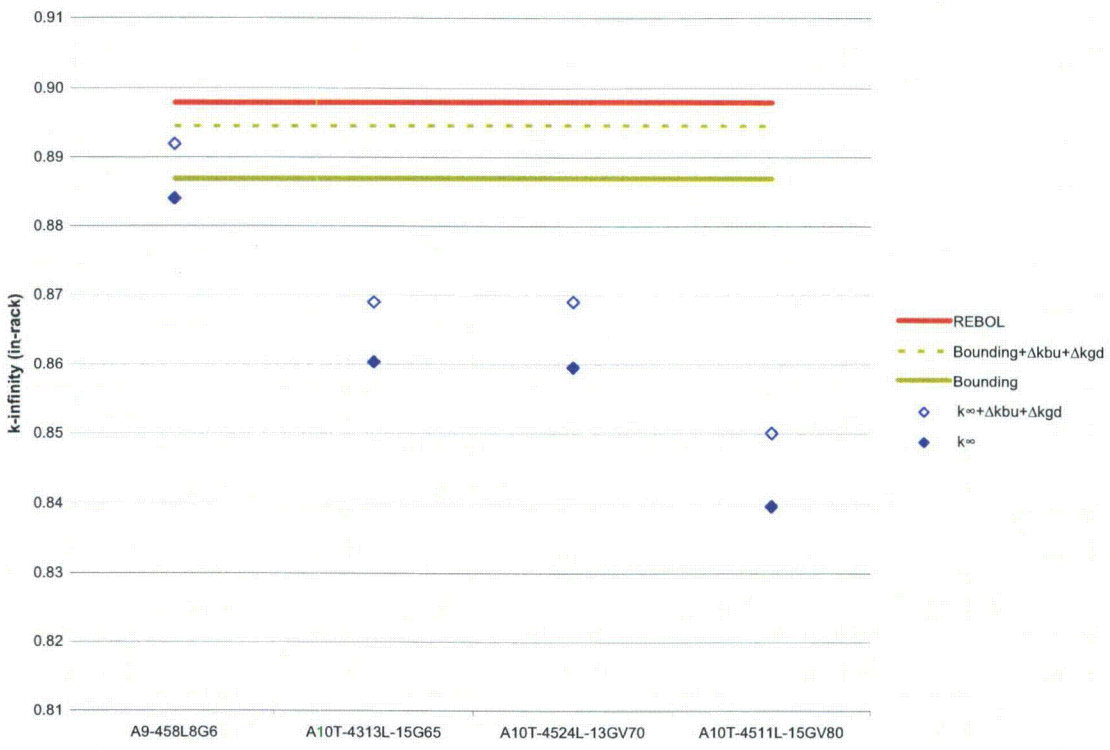

Figure RAI-11.2: Most Reactive Intermediate Lattices (96" to 126")

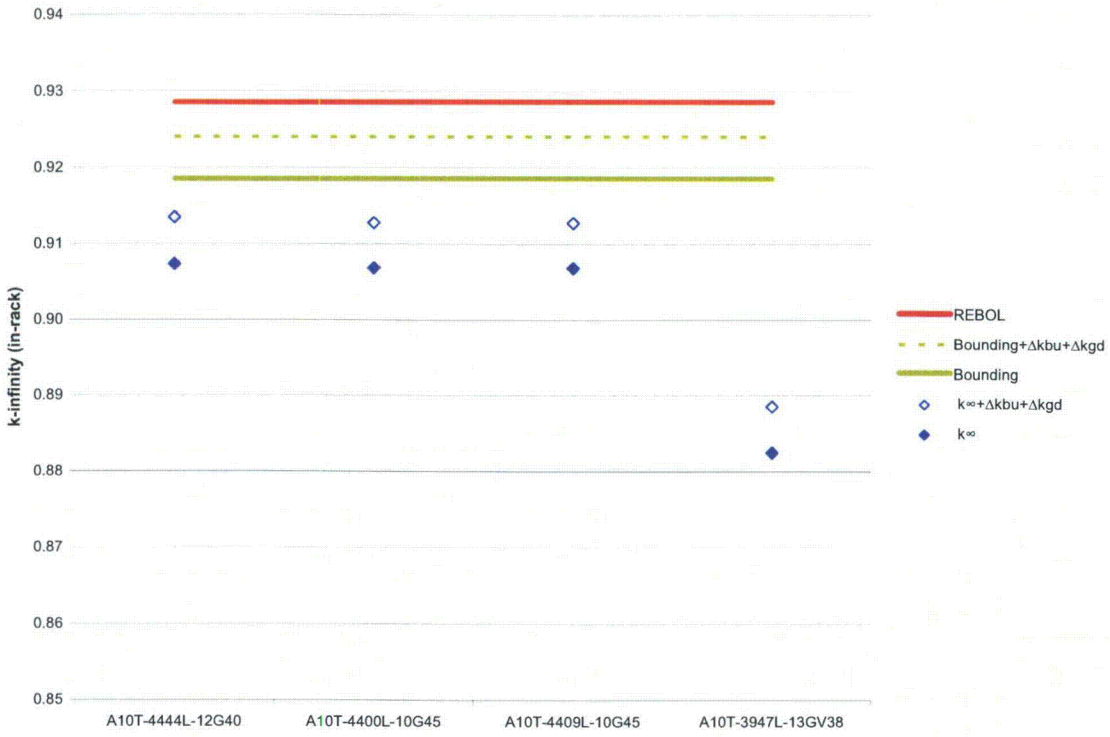

Figure RAI-11.3: Most Reactive Top Lattices (above 126")

2.8 *Request for Additional Information No. 12*

ANP-2843(P) (proprietary), Table 2.1, Section 3. This part of Table 2.1 describes the parameters for lattice designs that are acceptable without further review. The description states minimum numbers of Gd rods and minimum Gd content in each rod, but does not specify maximum values for either or the range of acceptable number of part-length rods or their permissible locations. The uncertainties associated with these design variations should be considered in the uncertainty analysis. The description should also describe where natural uranium blankets may be used.

Provide a more complete description of the acceptable range of lattice designs or justify not doing so.

Response:

The acceptance criteria presented in Table 2.1 are specific to future ATRIUM-10 assemblies only and will apply to both the Unit 1 pool and the Boraflex and NETCo insert regions of the Unit 2 pool.

Maximum values are not specified for the number of Gadolinia rods nor the maximum Gadolinia weight percent since an increase in the Gadolinia content results in a decrease in the peak reactivity. This is illustrated in Figure RAI-22.2 which shows a significant decrease in the peak reactivity for a lattice as the Gadolinia concentration is increased.

The number and location of part-length fuel rods is a function of the fuel design / product line. The ATRIUM-10 design has eight (8) part-length fuel rods in fixed locations. Any changes to the number of part length rods and their locations / lengths would be coincident with the introduction of a new fuel product line (e.g. ATRIUM 10XM). This necessitates the generation of a new criticality analysis for that new fuel product line.

There are no restrictions with respect to natural-U blankets since the lower reactivity inherent in their use was not credited in ANP-2843(P).

2.9 *Request for Additional Information No. 14*

ANP-2843(P) (proprietary), Section 3.0 includes a listing of design criteria applicable to the spent fuel storage evaluation. GDC 5, GDC-62. "Prevention of Criticality in Fuel Storage and Handling," and 10 CFR 50.68(b)(7) are missing from the list.

Confirm that the analysis documented in ANP-2843(P) is compliant with these requirement sources.

Response:

The analysis documented in ANP-2843(P) complies with the applicable requirements of GDC-5, GDC-62, and 10CFR50.68(b)(7). This is discussed in more detail in the response to RAI-7 and RAI-36.

2.10 *Request for Additional Information No. 16*

ANP-2843(P) (proprietary), Table 4.1. The fuel rod description includes both a theoretical density and a pellet void volume percent. Is the effective pellet density the combination of the two (i.e., effective density is 95.10 percent of theoretical density)?

Clarify how the pellet void volume percent is used.

Response:

The density specified in Table 4.1 is the actual pellet density. In the determination of the column or stack density, the void volume is included. The void volume represents the volume difference relative to a stack of cylinders (e.g. includes differences from a cylindrical volume caused by chamfers and depressions on the pellet ends). The reviewer is correct in that the effective column or stack density is a combination of these two components or 95.10% percent of theoretical density. Stack density is also addressed in the response to RAI-34(e).

2.11 *Request for Additional Information No. 17*

ANP-2843(P) (proprietary), Table 4.1. The fuel channel description implies that the fuel channels are a uniform thickness. At some plants. a fuel channel may have multiple wall thicknesses. If the LSCS reactor uses fuel channels that have multiple wall thicknesses, the modeling simplification should be stated and the impact of the simplification on the analysis should be quantified.

Confirm that the actual fuel channels have a uniform wall thickness.

Response:

For the ATRIUM-10 design, Exelon has chosen to use channels with a uniform wall thickness in the LaSalle Unit 1 and 2 reactors. However, storage of fuel with an advanced channel (i.e. varying wall thickness) is bounded by the 100 mil thickness channel used in the criticality safety analysis.

As shown in the response to RAI-10, in-rack reactivity increases with increasing wall thickness (and resultant increase in channel wall cross-sectional area). The increase in wall thickness results in an increase in channel mass and wall cross-sectional area which in turn results in water displacement. The AREVA ATRIUM-10 advanced channel design is thicker at the corner with a thinner wall along the side. As shown below, the advanced channel cross-sectional area falls between the 80 mil and 100 mil channels evaluated in RAI-10.

Table RAI-17.1: Channel Cross-Sectional Area

Channel Wall Thickness (mil)	Channel Wall Cross-Sectional area (in^2)	Channel Type
100[1]	2.074	uniform
[ ]	[ ]	advanced
80	1.657	uniform

[1] At LaSalle, the 100 mil uniform fuel channel is currently being used with the AREVA ATRIUM-10 fuel assembly.

Some previously manufactured assemblies in the LaSalle Unit 1 and 2 spent fuel pools used a fuel channel with varying wall thickness regions, (i.e. the GE14 assemblies). The CASMO-4 reactivity comparisons shown in Appendix B of ANP-2843(P) explicitly model the changes in fuel channel thickness for the GE14 assemblies as well as the use of uniform 80 mil channels for some of the older assembly types. Similar to the response to RAI-10, previously manufactured assemblies without fuel channels will be less limiting than when the fuel channel is installed.

2.12 *Request for Additional Information No. 18*

ANP-2843(P) (proprietary), Table 4.2. No tolerance is provided for the insert wing length. A footnote is provided that implies that the wing length is modeled as longer than it really is. What is the tolerance on the wing length and what is the impact of the modeling simplification used?

Provide the tolerance on the insert wing width. If appropriate, include this tolerance in the uncertainty analysis documented in Section 6 of ANP-2843(P). Evaluate the impact of the modeling simplification stated in the footnote on Page 4-4 of ANP-2843(P).

Provide a description of the wing material model. Justify any modeling simplifications made.

Response:

As shown in Attachment 4 of the Reference 2 licensing amendment request (Drawing NET-259-NSI-LS2-A-02 Revision 3), the insert is comprised of a uniform neutron absorbing material with a pre-fabrication width of 12.155 ± 0.010" and a post-fabrication wing length of 5.93". In its final form, the insert has rounded corners in the center and on the 2 ends. Both the CASMO-4 and KENO V.a models use a slightly longer than actual wing length. This is done to represent the curvature at the ends of the insert with a simple geometry. As described in Table 4.2 of ANP-2843(P) the wing length is modeled as 6.00" in CASMO-4 and 5.98" in KENO V.a . In both models a 90° bend angle is assumed in the center of the insert. Applying the nominal thickness of 0.065", then 11.935" (i.e. 2*6.00" – 0.065" = 11.935") and 11.895" (i.e. 2*5.98" – 0.065" = 11.895") of the 12.155" wide neutron absorbing material is actually used in the CASMO-4 and KENO V.a computer models, respectively. This is conservative for both models because neutron absorbing material has been excluded.

No tolerance has been applied to the length of the insert wing because the modeled length is less than the minimum pre-fabrication width (12.145"). The effect of the insert wing thickness tolerance has been evaluated in Table 6.3 of ANP-2843(P) and in Table RAI-34.1 in the response to RAI-34(f).

2.13 *Request for Additional Information No. 19*

ANP-2843(P) (proprietary), Figure 4.2. Due to the off-center location of the water hole, assembly rotations should have been evaluated in conjunction with assembly groupings.

Provide more detailed discussion of assembly rotation studies performed so that the NRC staff may confirm that this issue was fully studied. What rotations and assembly locations were evaluated?

Response:

With the insert in the lower right hand corner, the four simple (0, 90, 180, and 270 degree) rotation scenarios have been evaluated on an infinite lattice basis. The zero degree rotation case (shown in Figure 4.2 of ANP-2843(P)) was selected as the base case because it was the most reactive of these four rotation scenarios. In addition, the five rotational combination scenarios shown in Figure RAI-19.1 were also investigated on an infinite lattice basis. Orientation 5 provided the highest reactivity result with less than a 0.001 Δk increase. In all instances the fuel assemblies were centered in the water region of the storage cells.

RAI-24 indicates that optimization studies should be performed for the accident scenarios. Translation studies for the rotated assembly are not required because the centered position already provides a near optimal water gap. The reactivity increase from the rotated assembly scenario (0.001 Δk) is small in comparison to the optimized missing insert scenario (0.003 Δk) discussed in the response to RAI-24.

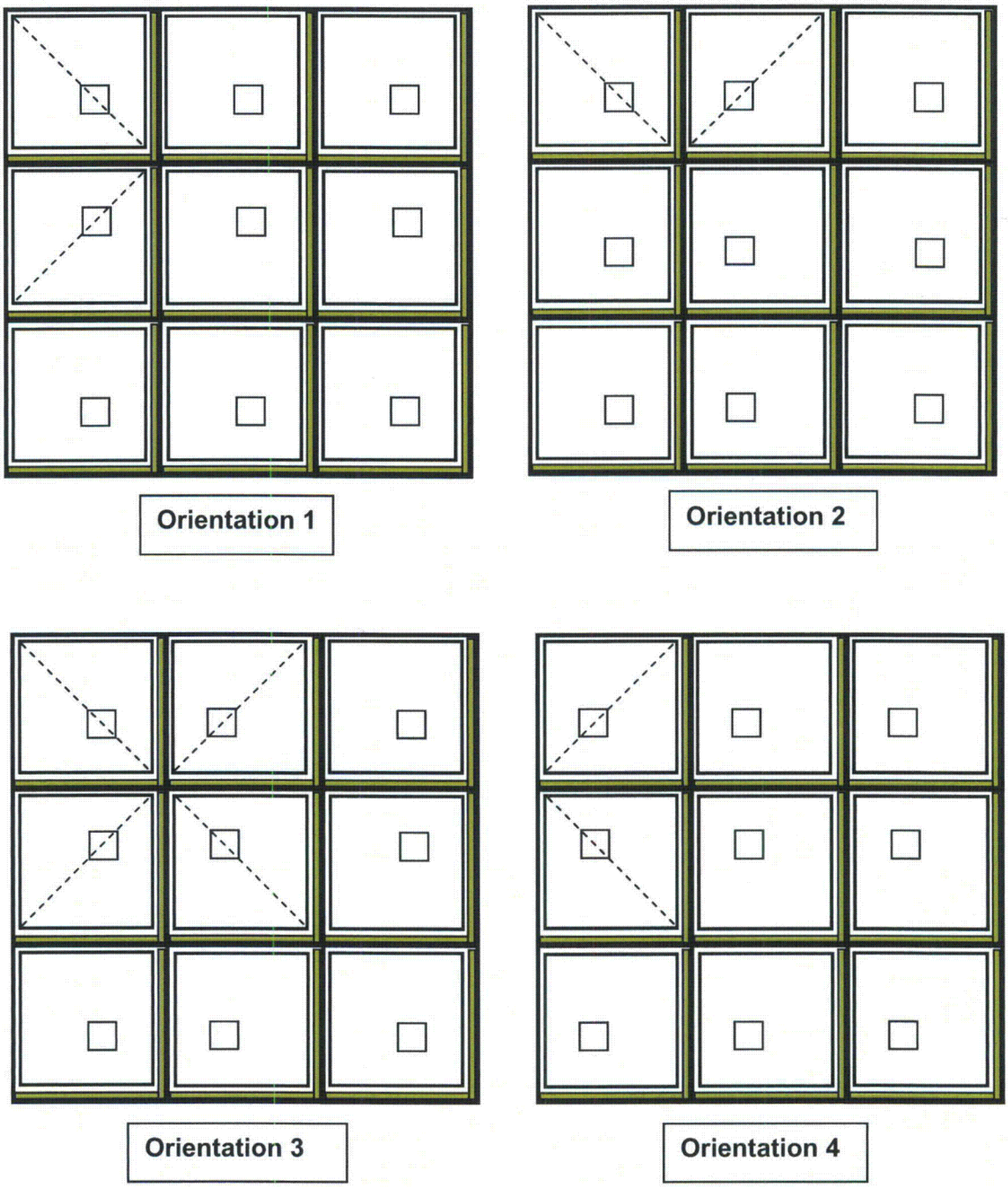

Figure RAI-19.1: Combined Assembly Rotation Scenarios

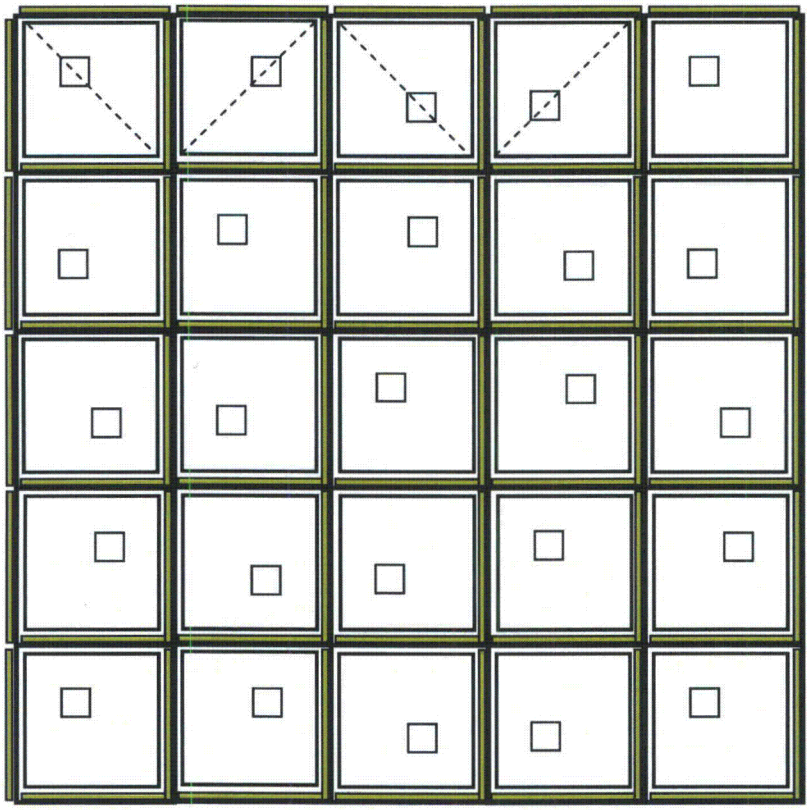

Orientation 5

Figure RAI-19.1: Combined Assembly Rotation Scenarios (continued)

2.14 *Request for Additional Information No. 20*

ANP-2843(P) (proprietary), Section 5.0. This section presents the calculation methodology. From reading the rest of the report, it looks like all CSAS25 calculations were for models with fresh fuel that had no Gd rods. All variations from these conditions were evaluated using CASMO-4. Additionally, some uncertainties documented in Section 6 were evaluated using CASMO-4.

Confirm the NRC staff understanding of the calculation methodology.

Response:

The NRC summation is generally correct [

]

Figure RAI-35.1 provides an overview of where KENO V.a and CASMO-4 are used in the analysis.

[1] [

] The adder of 0.002 is documented in the footnote to Table 6.3 of ANP-2843(P) and Table RAI-34.1 of this document.

2.15 *Request for Additional Information No. 21*

ANP-2843(P) (proprietary), Section 5.0, page 5-2, 1st bulleted item. This item states that in-core depletions were performed at certain void percentages. As is noted near the top of page 6-2, the limiting in-rack k_∞ values were calculated for each lattice using a particular percent void history during depletion. It is not clear that some other value would not result in a higher value. Consequently, there is some uncertainty associated with this simplified analytical approach that has not yet been quantified.

Justify the use of only the particular void histories. Note that while these values may be sufficient for reactor safety analysis, additional calculations may be needed for criticality safety analysis.

Response:

Additional justification is provided to show that in-core depletion at the EMF-2158(P)(A) void history levels are sufficient for criticality safety analysis. Figure RAI-21.1 shows the results of a sensitivity evaluation with respect to the in-core depletion void history and its effect on the in-rack lattice k_∞. For the limiting lattices (i.e. both the previously manufactured and the reference bounding lattices) in this analysis the void history conditions used either produced the maximum k_∞ condition or the difference between the void history used and the maximum is not significant. This is demonstrated below.

The limiting previously manufactured lattices are identified in Table B.1 of ANP-2843(P):

- For the bottom and intermediate zones (zero to 126") the ATRIUM-9 458L8G6 lattice depleted with [

  ]

- For the top zone (126" to 149"), the ATRIUM-10 (top) 4444L12G40 lattice depleted with [

  ]

The reference bounding lattices are identified in Table B.1 of ANP-2843(P):

- For the bottom zone (zero to 96") the ATRIUM-10 (bottom) 457L10G60 lattice achieves a maximum k_∞ at [

  ]

  is not significant (less than 0.0001 Δk).

- For the Intermediate zone (96" to 126") the ATRIUM-10 (top) 457L10G60 lattice achieves a maximum k_∞ at [

  ] is not significant (about 0.0001 Δk).

- For the top zone (126" to 149") the ATRIUM-10 (top) 447L10G35 lattice achieves a maximum k_∞ at [

  ] value is bounding for the top elevation zone.

Figure RAI-21.1: Impact of Void History Depletion on In-Rack k_∞

2.16 *Request for Additional Information No. 22*

ANP-2843(P) (proprietary), Section 5.0, page 5-2, 4th bulleted item. This item states that a 0.01 Δk margin is built into the REBOL lattices to account for calculational and depletion uncertainties. It is not clear that this 0.01 Δk margin is adequate. This margin needs to cover bias and bias uncertainty associated with:

- *fuel actinide composition calculations,*
- *fission product composition calculations,*
- *Gd depletion calculations, and*
- *keff calculations (nuclear data errors)*

The "depletion" uncertainty (discussed in Section D.3.3) extracted from Table 2.2 of EMF-2158(P)(A) is for boiling-water reactor (BWR) simulator code (i.e. CASMO4+MICROBURN-B2) validation. It is not clear that this uncertainty is applicable to standalone CASMO-4 models used to calculate in-rack k_∞.

Provide additional justification for the 0.01 Δk margin used to account for calculational and depletion uncertainties.

Response:

Additional justification for the 0.010 Δk margin is provided based on usage of the 5% reactivity decrement as a result of fission product build up and the change in actinide concentrations from BOL to the point at which peak reactivity is reached. The approach presented here is a conservative application of the 5% reactivity decrement approach suggested in the Kopp memo (Reference D.1 of ANP-2843(P)).

To quantify the change in reactivity associated with fission products and actinide composition, evaluations of the ATRIUM-10 reference bounding lattices were performed using the CASMO-4 depletion code. These lattices are identified in Table B.1 of ANP-2843(P) and the evaluation is performed at 4 °C, which is the limiting temperature condition. All lattices are depleted in-core and then evaluated in the LaSalle Unit 2 storage rack configuration (including inserts).

BOL solutions for each lattice were completed by removing the gadolinium from the lattices and maintaining the same uranium number densities in the lattice. This results in a higher BOL reactivity or k_∞. The decrease in reactivity as a result of changes in actinide and fission product

inventory during burnup from BOL to actual peak reactivity is determined by subtracting the peak in-rack k_∞ from the BOL no gad in-rack k_∞. This decrement also includes the associated reactivity decrease associated with residual gadolinia.

To assess an additional penalty for residual gadolinia content, additional CASMO-4 calculations were performed in which the in-core depletion restart was read and the residual gadolinia number densities were set to essentially zero (i.e. 1.0E-14) in in-rack calculations. Figure RAI-22.1 illustrates the process to assess the reactivity decrement from BOL to peak reactivity, and the effect of the residual gadolinia at peak reactivity in the in-rack configuration.

Based on the calculation process illustrated in Figure RAI-22.1, 5% of the burn-up reactivity decrement (Δkbu) and 5% of the residual gadolinia reactivity change (Δkgd) are tabulated in Table RAI-22.1 for the reference bounding lattices. Also tabulated is an adjusted k_∞ in which both the burn-up and gadolinia reactivity impacts are added to the peak reactivity value which allows comparison to the actual REBOL reactivities.

These results demonstrate that the 0.010 Δk added to the k_∞ of the reference bounding lattices when defining the enrichment level of the REBOL lattices is sufficient to account for the code bias and uncertainty associated with the fuel depletion and nuclear data library errors because the maximum depletion uncertainty for the reference bounding lattices is 0.0078 Δk, (i.e. less than 0.010 Δk).

It is noted that this process will produce a larger penalty as the gadolinia content increases (either the number of rods or the concentration). However, increasing the gadolinia content within a given lattice will also decrease the peak in-rack k_∞ of a lattice as shown in Figure RAI-22.2 and Table RAI-22.2. Table RAI-22.2 shows the depletion penalty for the ATRIUM-10 lattices with gadolinia listed in Table B.2 of ANP-2843(P) and has been added to demonstrate that these larger penalties are not sufficient to make an actual lattice more limiting than the reference bounding lattice. For example, the largest adjustment penalty with this method (0.0105) occurs for an intermediate zone lattice with 15 rods containing 8 wt% Gd2O3. Although this lattice produces a higher depletion penalty, the adjusted k_∞ for this lattice is ~0.044 Δk less than the in-rack k_∞ for the adjusted bounding lattice (0.8946-0.8501).

Table RAI-22.1: Reactivity Decrement for Bounding Lattices

	Peak k-inf [1]	BOL k_{nogad}	Δkbu (0.05*Δk)	Δkgd (0.05*Δkg)	Δkbu + Δkgd	k_{adj} *
Bottom Zone						
Bounding Lattice	0.8843	1.0201	0.0068	0.0010	0.0078	0.8921
REBOL Lattice						0.8947
Intermediate Zone						
Bounding Lattice	0.8869	1.0216	0.0067	0.0010	0.0077	0.8946
REBOL Lattice						0.8977
Top Zone						
Bounding Lattice	0.9186	1.0160	0.0049	0.0007	0.0055	0.9241
REBOL Lattice						0.9287

* kadj = Peak k + Δkbu + Δkgd (not applied to REBOL lattice)

Table RAI-22.2: Reactivity Decrement for Limiting ATRIUM-10 Lattices

	Peak k-inf [1,2]	BOL k_{nogad}	Δkbu (0.05*Δk)	Δkgd (0.05*Δkg)	Δkbu + Δkgd	k_{adj} *
Bottom Zone						
A10B-4399L-12G65	0.8706	1.0110	0.0070	0.0010	0.0080	0.8786
A10B-4510L-13G75	0.8634	1.0160	0.0076	0.0010	0.0086	0.8721
A10B-4537L-13GV70	0.8573	1.0177	0.0080	0.0014	0.0094	0.8668
A10B-4538L-13GV80	0.8445	1.0176	0.0087	0.0016	0.0102	0.8547
Bounding Lattice	0.8843	1.0201	0.0068	0.0010	0.0078	0.8921
Intermediate Zone						
A10T-4313L-15G65	0.8604	1.0053	0.0072	0.0014	0.0086	0.8690
A10T-4524L-13GV70	0.8596	1.0183	0.0079	0.0015	0.0094	0.8689
A10T-4511L-15GV80	0.8396	1.0176	0.0089	0.0016	0.0105	0.8501
Bounding Lattice	0.8869	1.0216	0.0067	0.0010	0.0077	0.8946
Top Zone						
A10T-4444L-12G40	0.9074	1.0146	0.0054	0.0008	0.0062	0.9136
A10T-4400L-10G45	0.9069	1.0121	0.0053	0.0007	0.0060	0.9128
A10T-4409L-10G45	0.9068	1.0117	0.0052	0.0007	0.0059	0.9127
A10T-3947L-13GV38	0.8825	0.9869	0.0052	0.0008	0.0061	0.8885
Bounding Lattice	0.9186	1.0160	0.0049	0.0007	0.0055	0.9241

* kadj = Peak k + Δkbu + Δkgd

Note: In the above tables, some numerical differences in the last significant digit occur due to rounding.

1 The Peak k-infinity values for the bounding lattices are the same as those in Table B.1 of ANP-2843(P) except that they are reported here to 4 significant digits.

2 The Peak k-infinity values for the limiting lattices are the same as those in Table B.2 of ANP-2843(P) except that they are reported here to 4 significant digits.

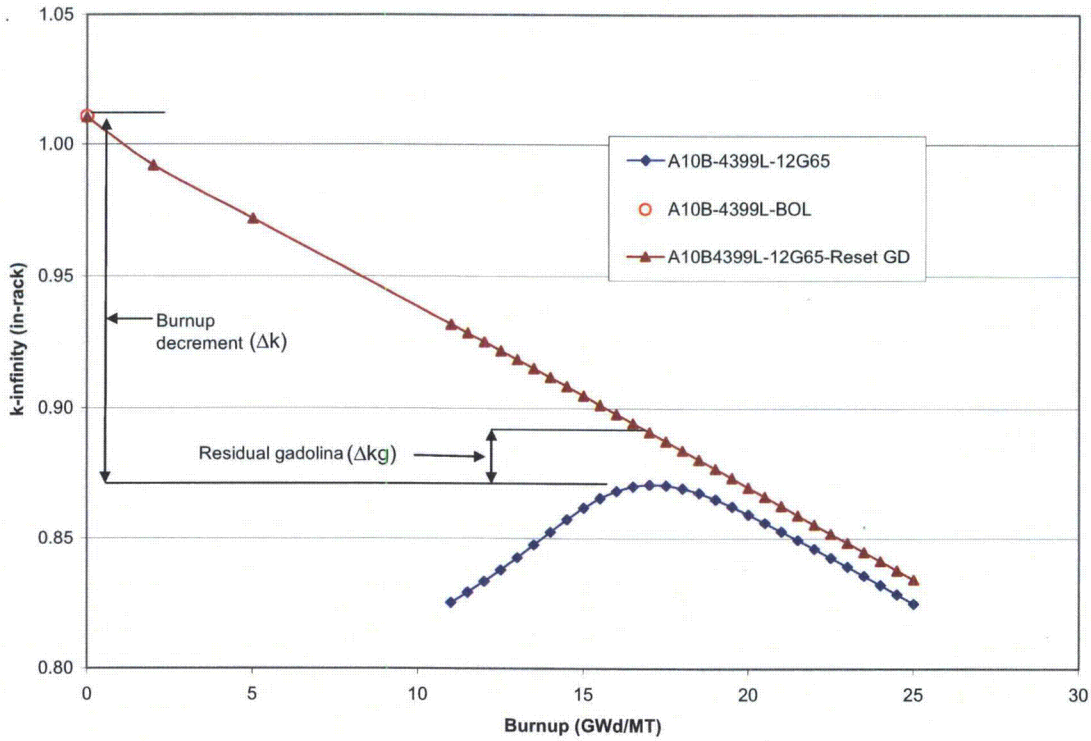

Figure RAI-22.1: Depletion Penalty Assessment

Figure RAI-22.2: LaSalle Unit 2 Storage Pool In-Rack k_∞ Comparison

2.17 *Request for Additional Information No. 23*

ANP-2843(P) (proprietary), Section 5.1, page 5-3, last paragraph. This text concludes that the CASMO-4 calculations performed for the evaluation are within the area of applicability (AOA) of the comparisons shown in Appendix D. All comparisons shown in Appendix D involve fresh fuel without Gd rods. The CASMO-4 depletion calculations which involve burned fuel compositions and Gd rods are clearly not within the AOA of the comparisons shown in Appendix D.

Revise the report to (1) more accurately and clearly describe the verification and validation of computational methods used and (2) to justify the extension of the AOA.

Response:

The paragraph at the end of Section 5.1 states:

> *For the CASMO-4 qualification, ATRIUM-10 fuel lattices were modeled using the LaSalle fuel storage rack geometry. Therefore, the CASMO-4 calculations performed for this evaluation are within the area of applicability of the comparisons shown in Appendix D.*

The primary intent of this statement is to identify that the Appendix D code-to-code comparisons are directly applicable to the in-rack calculations documented in the main body of the report (i.e. the same in-rack geometry model was used for both). The validity of the area of applicability as documented in Appendix D is addressed in the responses to RAI-42 and RAI-43.

One of the primary purposes of Appendix D [

] The Appendix D comparisons are sufficient to demonstrate that geometric, thermal, and U-235 enrichment differences are treated similarly between the two codes.

Prior to the definition of the REBOL lattices, the CASMO-4 code was used to compare lattice reactivity values at projected maximum reactivity conditions. These maximum reactivity results are all subject to very similar uncertainties, such as gadolinia and U235 depletion, fission product generation, isotopic transmutation, code calculational uncertainties, etc. The approach

taken in the ANP-2843(P) analysis is not to quantify these depletion uncertainties with the goal of including them as part of the $k_{95/95}$ calculation, but instead the analysis uses a conservative adder in the definition of the REBOL lattices. The adequacy of this adder is addressed by comparing to estimates of the depletion uncertainty such as the one provided in Section D.6 of ANP-2843(P) or the alternate approach defined in the response to RAI-22.

2.18 *Request for Additional Information No. 24*

ANP-2843(P) (proprietary), Section 6.5 covers abnormal and accident conditions. One condition evaluated was the placement of an assembly next to the side of a fuel storage rack module. The analysis of this configuration should have been for an assembly placed in a corner formed by three rack modules. Further, the analysis should have optimized the "normal" conditions to maximize the k_{eff} value for the accident condition. For example, k_{eff} might be increased if the three assemblies are moved toward the assembly that is placed next to the racks, or if some or all of the four assemblies involved are not installed in fuel channels.

Another condition evaluated was a missing insert. Again, the normal conditions should have been revisited to maximize the impact of the missing insert. This might include moving some of the surrounding assemblies toward the cell with the missing insert.

Confirm that the normal conditions were re-optimized to maximize k_{eff} for the abnormal and accident conditions.

In addition to a missing insert, the abnormal conditions discussion should address:

- *The potential for and, if appropriate, the impact of loss of boron due to corrosion, erosion, and mechanical wear.*
- *Misassignment or miscalculation of lattice k_∞ value.*
- *Comparison of lattice k_∞ value with the wrong zone-dependent limit.*
- *Placement of an assembly in the wrong fuel storage rack region.*

Address the potential for these abnormal conditions and, where appropriate, incorporate into the criticality analysis.

Response:

The misload scenario described here and pictured in RAI-5 for an assembly placed in a corner formed by three rack modules (as opposed to placement of an assembly next to the side of a fuel storage rack module) can occur at numerous places outside of the storage cell locations. However, due to the physical configuration of the pool storage array, any such misloading of an assembly in the corner between storage racks is limited to a configuration where the corner extends for a maximum of only five rows or five columns of stored fuel in the east-west or north-south directions (see Figure RAI-24.1). This limiting configuration (using a channeled and unchanneled fuel assembly in the corner) has been evaluated with the face adjacent assemblies in the center of the water region (maximizing reactivity) and the misloaded assembly in close proximity to the corner. This evaluation produced a case with a 0.0016 Δk increase in k-eff.

Further optimization of assembly position was not evaluated because neutron capture in the water region surrounding the misloaded assembly will ensure this scenario is less limiting than the optimized missing insert scenario.

The missing insert scenario has been evaluated under the five optimized conditions listed below. Condition 3 with the unchanneled assembly near the center of the cell (see Figure RAI-24.2) was found to be the most reactive situation with a final k-inf 0.0002 Δk higher than found in the original calculation. There was sufficient rounding margin included with the result reported in ANP-2843(P) that the limiting accident worth of 0.003 Δk is still supported. It is now confirmed that the limiting accident scenarios have been evaluated with effort to maximize the reactivity.

Each of the following conditions represents a series of calculations used to define the most limiting combination.

Condition 1: Missing insert cell assembly is unchanneled and is evaluated in multiple locations between the lower right corner of the cell and the center of the cell. All surrounding assemblies are channeled and centered.

Condition 2: Missing insert cell assembly is channeled and is evaluated in multiple locations between the lower right corner of the cell and the upper left corner of the cell. All surrounding assemblies are channeled and centered. This is similar to Condition 1 except that the assembly in the missing insert cell is channeled and the assembly is moved past the center of the cell.

Condition 3 (Limiting Condition): Missing insert cell assembly is unchanneled and is evaluated in multiple locations between the lower right corner of the cell and the center of the cell. All surrounding assemblies are channeled and centered except for the 2 channeled assemblies in the cells that are face adjacent to the missing insert cell (i.e. faces with no insert wing adjacent to the missing insert cell). These two face adjacent assemblies are positioned to have the closest possible proximity to each other. This nearly centered position creates the limiting condition and is illustrated in Figure RAI-24.2.

Condition 4: Missing insert cell assembly is channeled and is evaluated in multiple locations between the lower right corner of the cell and the center of the cell. All surrounding assemblies are channeled and centered except for the 2 in face adjacent cells. These are positioned to have the closest possible proximity to each other. This is the same as Condition 3 except that the assembly in the missing insert cell is channeled.

Condition 5: All surrounding assemblies are channeled and centered. The 3 fuel assemblies that are most affected by the missing insert are moved to have the closest possible proximity. The fuel channel is then removed from the assembly in the missing insert cell, followed by a face adjacent assembly, and then finally the second face adjacent assembly. When the fuel channel is removed each assembly is moved to contact the cell wall.

The loss of Boron-10 scenario has been accounted for in the base calculation since the minimum areal density of 0.0086 g/cm^2 was used. The potential for mechanical wear is addressed in the response to RAI-4.

The misassignment, miscalculation, or incorrect comparison of lattice k_∞ values is not an accident or abnormal condition. This type of error is addressed in the response to RAI-13.

As shown in Attachment 2 (the LaSalle Unit 1 and Unit 2 proposed spent fuel pool Technical Specification) of the LAR, the reactivity of all future fuel assemblies in both spent fuel pools will be restricted to the limits of the ANP-2843(P) criticality analysis. As shown in Table B.1 of ANP-2843(P) and discussed in the responses to RAI-28 and RAI-37, all previously manufactured fuel assemblies are bound by this same limit. Therefore, no higher reactivity assembly is approved for storage in any region of the LaSalle Unit 2 spent fuel pool.

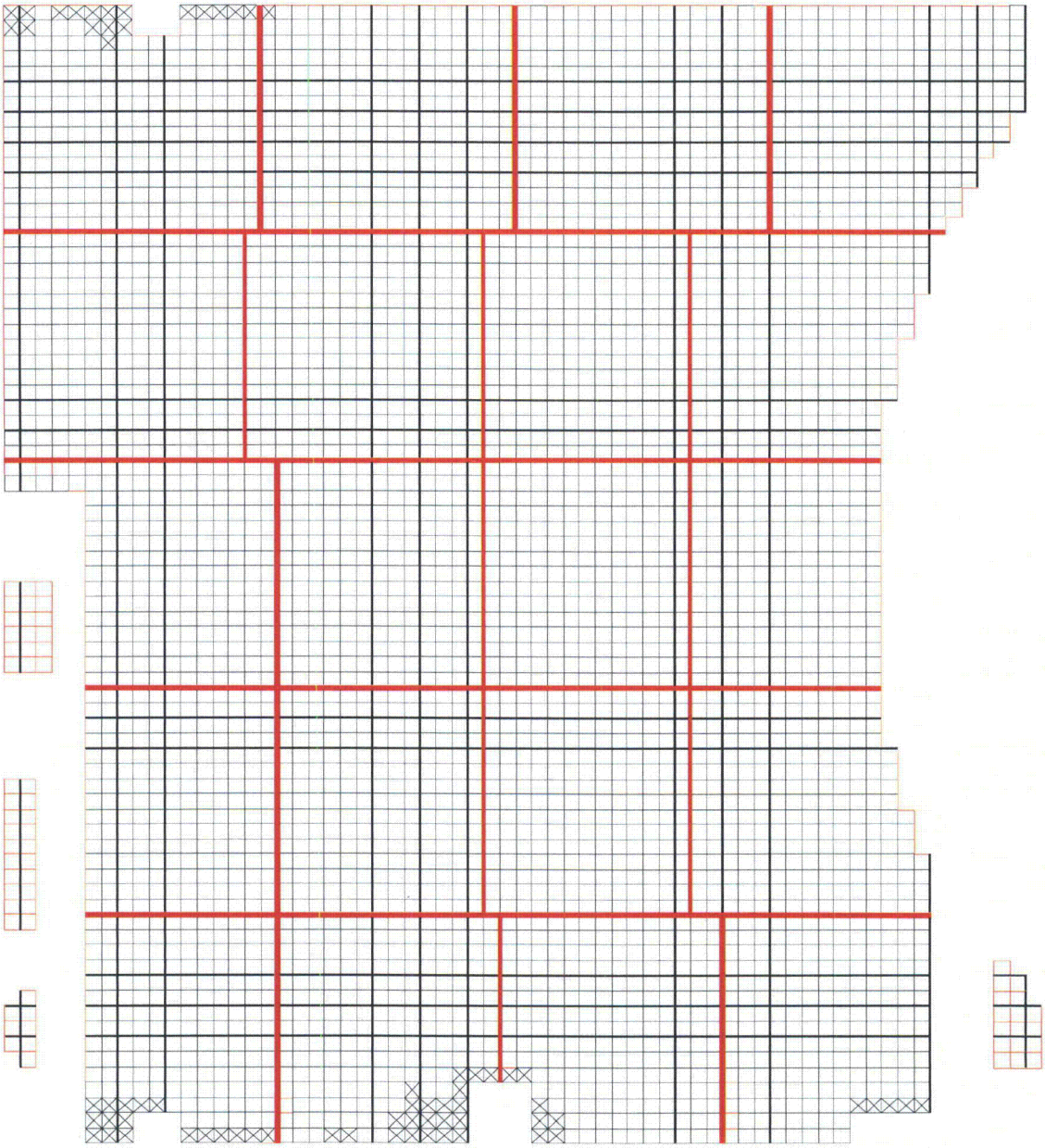

----------> N

☒ = Location not accessible for fuel placement.

Figure RAI-24.1: LaSalle Unit 2 Spent Fuel Pool

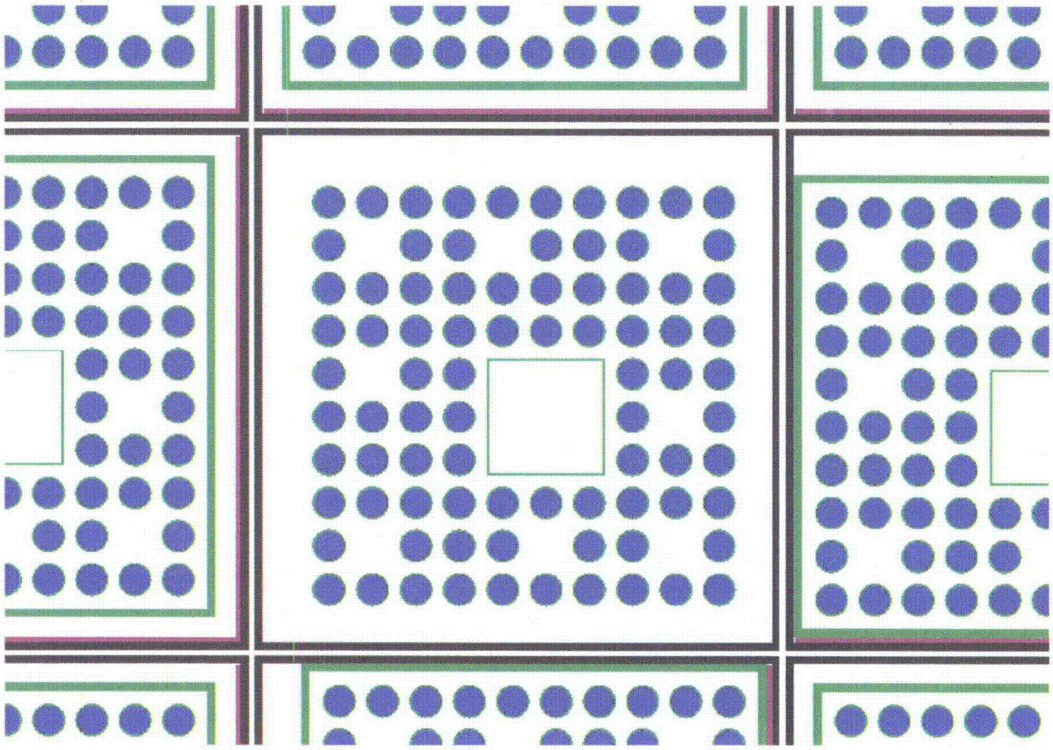

Figure RAI-24.2: Limiting Missing Insert Condition

2.19 *Request for Additional Information No. 25*

ANP-2843(P) (proprietary), footnote at the bottom of page 6-6 -Provide a reference supporting this claim or perform the analysis.

Response:

The $k_{95/95}$ calculation in Section 6.6 of ANP-2843(P) is specific to the ATRIUM-10 fuel assembly. This general observation is included to assert that one of the previously manufactured fuel types will not have a sufficiently high manufacturing tolerance uncertainty value to become more limiting in a $k_{95/95}$ calculation than the analyzed ATRIUM-10 assembly. From the tables in Appendix B of ANP-2843(P), ATRIUM-9 lattice A9-458L8G6 is the next most reactive non-ATRIUM-10 lattice. The following table compares the reactivity values of the limiting ATRIUM-10 and ATRIUM-9 lattices.

Table RAI-25.1: Limiting ATRIUM-9 to Bounding Lattice Comparison (in-rack)

Elevation Zone	k_∞ of the ATRIUM-10 Reference Bounding Lattice	k_∞ of the Next Limiting Non-ATRIUM-10 Lattice (A9-458L8G6)	Margin (Δk_∞)
Top	0.919	0.884	0.035
Intermediate	0.887	0.884	0.003
Bottom	0.884	0.884	0.000

Given the more reactive condition of the ATRIUM-10 assembly evaluated in this analysis the combined manufacturing tolerance uncertainty of an ATRIUM-9 assembly would need to be higher than the 0.0105 Δk used in this analysis. The margin is significantly larger for the other previously manufactured assembly types (this is illustrated in the response to RAI-28).

Comparison of fuel specific manufacturing tolerance uncertainty values has been performed between the ATRIUM-9 and ATRIUM-10 assembly types. This comparison shows that the limiting ATRIUM-9 design has a lower combined manufacturing tolerance uncertainty than the ATRIUM-10. Therefore, the ATRIUM-10 manufacturing tolerance uncertainty used in the ANP-2843(P) analysis bounds the other previously manufactured fuel in the LaSalle spent fuel pools.

2.20 *Request for Additional Information No. 26*

ANP-2843(P) (proprietary), Section 6.6, last paragraph, last sentence. The bias and bias uncertainty associated with burned fuel calculations has not been adequately incorporated into the calculation of $k_{95/95}$. Consequently, direct comparison of REBOL lattice k_∞ values with bounding lattice k_∞ values is not sufficient to reach the stated conclusion.

Incorporate the bias and bias uncertainty associated with burned fuel calculations into the analysis.

Response:

The CASMO-4 code bias and uncertainty with respect to fuel depletion is included in ANP-2843(P) through the use of the 0.010 Δk adder in the definition of the REBOL lattices. A CASMO-4 code bias is not used on the REBOL lattice results since these lattices are explicitly modeled within KENO. The adequacy of the 0.010 Δk adder is addressed in Appendix D of ANP-2843(P). Additional justification of this adder is included in the response to RAI-22.

2.21 *Request for Additional Information No. 27*

ANP-2843(P) (proprietary), Section 6.7 includes a statement that uniform rod enrichment distributions are more reactive than actual rod enrichment distributions by 0.005 to 0.007 Δk.

Provide a reference or describe what was done to support this claim. In particular, was the increased reactivity checked in fuel storage rack geometry? Is this statement true for assemblies with Gd rods burned to peak reactivity?

Response:

These results are based upon comparison of the maximum CASMO-4 in-rack k_∞ values of high reactivity ATRIUM-10 lattices (high lattice average enrichment levels and low gadolinia concentrations). The k_∞ values were defined by in-core depletion followed by in-rack solutions to obtain the maximum in-rack value. The distributed enrichment cases used lattices similar to the reference bounding lattices. The uniform enrichment cases were identical to the distributed case except the U235 enrichment level was changed to the lattice average enrichment in all fuel rods. The gadolinia was the same for both cases. Therefore, these are in-rack results for cases depleted with gadolinia to peak reactivity.

2.22 *Request for Additional Information No. 28*

ANP-2843(P) (proprietary), Section 6.8 - It is not clear how the conclusion reached in this section will be used. Does the applicant intend to assume all fuel already stored in the Unit 1 and Unit 2 spent fuel storage racks is bounded by the ATRIUM-10 lattices without checking the lattice k_∞ values? The text claims that the ATRIUM-10 lattices used in the evaluation can reasonably represent past assembly fuel types. It is not clear how the term "reasonably represent" can be consistent with the 10 CFR 50.68 requirement that the k_{eff} of the spent fuel storage racks loaded with fuel of the maximum fuel assembly reactivity must not exceed 0.95, at a 95 percent probability, 95 percent confidence level.

Describe the process, consistent with the 10 CFR 50.68(b)(4) requirement, that will be used to determine that the current inventory of spent fuel is acceptable for storage in the modified racks.

Response:

The statement sited in the RAI above is from the following sentence:

> *It then follows that the ATRIUM-10 lattices used in this evaluation can reasonably represent past assembly fuel types.*

This statement in the report is unclear and does not fully convey the desired intent. Specifically, this statement was intended to address that a criticality analysis using an infinite array of ATRIUM-10 lattice types (i.e. 10x10 geometry) will bound a mixed geometry array that includes the previously manufactured fuel types. It was not meant to convey that a full screening of the previously manufactured types was not performed. To fully answer this RAI, the response is divided as follows: 1) details of the screening for all previously manufactured fuel types, and 2) ability of the criticality analysis to bound the mixed geometries found in the spent fuel pool.

<u>Screening of Previously Manufactured Fuel</u>

Section 6.8 relies upon an evaluation of all previously manufactured assemblies in the LaSalle Unit 1 and Unit 2 SFPs. Appendix B of ANP-2843(P) summarizes the results of this evaluation by providing the k_∞ for the most limiting lattice result for each fuel type and axial elevation zone. This response provides additional detail on this characterization by providing results for

essentially all lattices in the SFP (note that some natural lattices and non-gadolinia lattices with enrichments below the REBOL lattices are not explicitly included in the following tables).

The previously manufactured assemblies were first screened based on enrichment and gadolinia content. A second screening was completed by evaluating both the peak in-core cold uncontrolled and controlled k_∞ for all lattices. The lattice reactivity was then ranked and the lattices with the highest reactivity were then evaluated in the storage rack configuration.

Tables RAI-28.1 and RAI-28.2 provide additional information with respect to the screening process and the evaluation of the 8x8 fuel. The cold in-core results of the ranking of the 8X8 assemblies are provided in Table RAI-28.1[1]. Based on the ranking results, the highest reactivity lattices were then evaluated in an in-rack configuration. These results are provided in Table RAI-28.2.

Tables RAI-28.3 and RAI-28.4 contain the in-core and the in-rack k_∞ of the ATRIUM-9 assemblies respectively.

Results for the GE14 assembly designs are presented in Tables RAI-28.5 and RAI-28.6.

The in-core screening results for the ATRIUM-10 gadolinia lattices are presented in Table RAI-28.7. The in-rack results for the ATRIUM-10 fuel are presented in Appendix B. As noted in the Introduction to Appendix B of ANP-2843(P), the previously manufactured fuel screening was performed for all fuel used at or manufactured for the LaSalle Unit 1 or Unit 2 reactors prior to July 2009. Fuel supplied after this date is required to meet the limitations of Table 2.1 of ANP-2843(P). The enriched lattices for the ATRIUM 10XM LTAs are explicitly included in Table B.3 of Appendix B.

These tables provide additional information which demonstrates that all fuel assembly designs previously delivered to the LaSalle Station have been evaluated and the most reactive lattice for each assembly type was reported in Appendix B. Demonstration that the reactivity of these

[1] The in-core calculations for the older 8x8 GE fuel tabulated in Table RAI-28.1 and used for initial screening were performed with a version of CASMO-3. The in-rack calculations for this fuel type were performed using CASMO-4. All other CASMO calculations in this report and in ANP-2843(P) were calculated with the CASMO-4 code.

previously manufactured assemblies is less than that of the reference bounding lattices confirms that the maximum fuel assembly reactivity has been used in the criticality safety analysis.

Mixed Geometry Consideration

The actual storage rack will contain a mixture of the previously manufactured fuel and future ATRIUM-10 designs. This results in a mixed array of GE 8x8, AREVA 9x9 (ATRIUM-9), GE 10x10 (GE14), and AREVA 10x10 (ATRIUM-10 and ATRIUM 10XM LTA) geometries.

The previously manufactured GE fuel designs provide significant margin between the limiting lattices to the corresponding reference bounding lattices. This is illustrated below:

Limiting of all as manufactured GE8x8 (From Tables B.1 and B.6 of ANP-2843(P)):

0.919 – 0.875 = 0.044 Δk	Margin to the Reference Bounding Lattice (top)
0.887 – 0.875 = 0.012 Δk	Margin to the Reference Bounding Lattice (intermediate)
0.884 – 0.875 = 0.009 Δk	Margin to the Reference Bounding Lattice (bottom)

Limiting of all as manufactured GE14 (From Tables B.1 and B.5 of ANP-2843(P)):

0.919 – 0.849 = 0.070 Δk	Margin to the Reference Bounding Lattice (top)
0.887 – 0.849 = 0.038 Δk	Margin to the Reference Bounding Lattice (intermediate)
0.884 – 0.842 = 0.042 Δk	Margin to the Reference Bounding Lattice (bottom)

Similarly, the AREVA 10x10 fuel designs show significant margin, as shown below:

Limiting of all as manufactured ATRIUM-10 (From Tables B.1 and B.2 of ANP-2843(P)):

0.919 – 0.907 = 0.012 Δk	Margin to the Reference Bounding Lattice (top)
0.887 – 0.860 = 0.027 Δk	Margin to the Reference Bounding Lattice (intermediate)
0.884 – 0.871 = 0.013 Δk	Margin to the Reference Bounding Lattice (bottom)

Limiting of all as manufactured ATRIUM 10XM LTAs (From Tables B.1 and B.3 of ANP-2843(P)):

0.919 – 0.880 = 0.039 Δk	Margin to the Reference Bounding Lattices (top)
0.887 – 0.852 = 0.035 Δk	Margin to the Reference Bounding Lattices (intermediate)
0.884 – 0.852 = 0.032 Δk	Margin to the Reference Bounding Lattices (bottom)

The bottom and intermediate reference bounding lattices were set based on the limiting ATRIUM-9 lattice. As shown below, the intermediate and top elevation zones show margin to their corresponding reference bounding lattices.

Limiting of all as manufactured ATRIUM-9 (From Tables B.1 and B.4 of ANP-2843(P)):

0.919 – 0.884 = 0.035 Δk	Margin to the Reference Bounding Lattice (top)
0.887 – 0.884 = 0.003 Δk	Margin to the Reference Bounding Lattice (intermediate)
0.884 – 0.884 = 0.000 Δk[1]	Margin to the Reference Bounding Lattice (bottom)

The ATRIUM-9 geometry in the in-rack configuration was explicitly included as a subset of the code-to-code comparison provided in Appendix D of ANP-2843(P). Lattice specific biases of the Appendix D data is addressed in the response to RAI-45. Specifically, Table RAI-45.1 shows that there is no significant difference in the weighted mean difference (Δkbar), total uncertainty (σ^2), variance (s^2), and square root of the pooled variance (Sp) for the different lattices.

This lack of lattice specific bias directly supports the use of the ATRIUM-10 geometry in a mixed lattice array also containing the ATRIUM-9 design. The acceptability of this approach can also be extended to the 8x8 and other 10x10 designs based upon the similarity between the designs and the margin to the reference bounding lattices (shown above).

[1] A small amount of margin exists when compared to the 4th significant digit. (0.0002 Δk, from values in Table RAI-28.4).

Table RAI-28.1: 8X8 Lattice Screening based upon Cold In-core Geometry

No.	Lattice	Max Uncontrolled k_∞	Max Controlled k_∞
1	8CIL071-NOG-100M-T	0.8728	0.7265
2	8CIL185-1G4.0/1G2.0-100M-T	1.1083	0.9338
3	8CIL185-2G5.0-100M-T	1.0927	0.9221
4	8CIL186-1G2.0-100M-T	1.1350	0.9592
5	8CIL230-4G5.0-100M-T	1.1183	0.9518
6	8CIL232-2G5.0/1G4.0-100M-T	1.1311	0.9630
7	8CIL232-3G2.0-100M-T	1.1759	1.0012
8	P8CRL319-6G3.0-100M-T	**1.2351**	**1.0570**
9	P8CQL071-8GE-100M-T	0.8469	0.6952
10	P8CQL319-2G4.0/6G3.0-100M-T	1.2022	1.0278
11	P8CQL319-6G3.0-100M-T	1.2240	1.0513
12	P8CQL340-2G4.0/7G3.0-100M-T	1.2199	1.0419
13	P8CQL340-7G3.0-100M-T	**1.2437**	**1.0680**
14	P8CQL340-7G4.0-100M-T	1.2201	1.0471
15	P8CQL071-NOG-100M-T	0.8763	0.7305
16	P8CWL071-NOG-100M-T	0.8620	0.7172
17	P8CWL071-10GE-100M-T	0.8225	0.6752
18	P8CWL320-4G4.0/3G3.0-100M-T	1.2052	1.0320
19	P8CWL320-7G3.0-100M-T	1.2199	1.0491
20	P8CWL323-5G4.0/4G3.0-100M-T	1.1977	1.0272
21	P8CWL323-9G3.0-100M-T	1.2171	1.0454
22	P8CWL326-10G4.0-100M-T	1.1955	1.0275
23	P8CWL326-5G5.0/4G4.0-100M-T	1.1832	1.0154
24	P8CWL326-6G5.0/4G4.0-100M-T	1.1828	1.0163
25	P8CWL326-9G4.0-100M-T	1.1956	1.0277
26	P8CWL327-4G5.0/5G4.0-100M-T	1.1859	1.0174
27	P8CWL327-9G5.0-100M-T	1.1729	1.0070
28	P8CWL337-2G4.0/9G3.0-100M-T	1.2110	1.0404
29	P8CWL337-9G3.0-100M-T	**1.2288**	**1.0558**
30	P8CWL337-9G4.0-100M-T	1.2066	1.0368
31	P8CWL338-10G4.0-100M-T	1.2041	1.0354
32	P8CWL338-2G4.0/7G3.0-100M-T	1.2173	1.0465
33	P8CWL338-4G5.0/5G4.0-100M-T	1.1938	1.0234
34	P8CWL338-7G3.0-100M-T	**1.2378**	**1.0650**
35	P8CWL339-2G4.0/5G3.0-100M-CECO	**1.2290**	1.0552
36	P8CWL339-4G4.0/3G3.0-100M-CECO	1.2215	1.0501
37	P8CWL339-7G4.0-100M-CECO	1.2132	1.0448
38	P8CWL345-5G5.0/4G4.0-100M-T	1.2099	1.0393
39	P8CWL345-9G4.0-100M-T	1.2175	1.0470
40	P8CWL346-4G5.0/3G4.0-100M-CEC	1.2077	1.0375

Table RAI-28.1: 8X8 Lattice Screening based upon Cold In-core Geometry (continued)

No.	Lattice	Max Uncontrolled k_∞	Max Controlled k_∞
41	P8CWL346-7G4.0-100M-CECO	1.2197	1.0506
42	P8CWL350-2G4.0/5G3.0-100M-CECO	**1.2353**	**1.0606**
43	P8CWL350-4G4.0/5G3.0-100M-CECO	1.2201	1.0492
44	P8CWL350-4G5.0/6G4.0-100M-T	1.2002	1.0313
45	P8CWL350-7G4.0-100M-CECO	1.2219	1.0527
46	P8CWL350-7G5.0/3G4.0-100M-T	1.1931	1.0257
47	P8CWL350-9G4.0-100M-CECO	1.2166	1.0487
48	P8CWL355-4G4.0/3G3.0-100M-CECO	**1.2305**	**1.0600**
49	P8CWL355-6G4.0/3G3.0-100M-CECO	1.2234	1.0527
50	P8CWL358-2G5.0/7G4.0-100M-CECO	1.2153	1.0511
51	P8CWL358-7G4.0-100M-CECO	**1.2274**	**1.0579**
52	P8CWL362-2G5.0/9G4.0-100M-T	1.2117	1.0396
53	P8CWL362-9G4.0-100M-T	**1.2314**	**1.0594**
54	P8CWL363-10G5.0-80M-CECO	1.1965	1.0323
55	P8CWL363-8G4.0-80M-CECO	1.2255	**1.0575**
56	P8CWL363-8G5.0-80M-CECO	1.2016	1.0368
57	P8CWL365-4G5.0/6G4.0-100M-T	1.2094	1.0407
58	P8CWL365-6G5.0/6G4.0-100M-T	1.2031	1.0336
59	P8CWL388-2G5.0/8G4.0-80M-CECO	1.2200	1.0540
60	P8CWL388-8G4.0-80M-CECO	**1.2381**	**1.0699**
61	P8CWL390-10G5.0-80M-CECO	1.2119	1.0471
62	P8CWL390-12G5.0-80M-CECO	1.2014	1.0377

Table RAI-28.2: Maximum in-Rack k_∞ For 8x8 Fuel

Lattice	in-rack k_∞
Bounding	0.8843
P8CWL388-8G4.0-80M-CECO	0.8752
P8CQL340-7G3.0-100M-T	0.8690
P8CWL350-2G4.0/5G3.0-100M-CECO	0.8646
P8CWL363-8G4.0-80M-CECO	0.8643
P8CWL355-4G4.0/3G3.0-100M-CECO	0.8637
P8CWL338-7G3.0-100M-T	0.8631
P8CWL362-9G4.0-100M-T	0.8621
P8CWL358-7G4.0-100M-CECO	0.8603
P8CWL339-2G4.0/5G3.0-100M-CECO	0.8588
P8CRL319-6G3.0-100M-T	0.8585
P8CWL337-9G3.0-100M-T	0.8569

Table RAI-28.3: ATRIUM-9B Lattice Screening based upon Cold In-core Geometry

No.	Lattice	Max Uncontrolled k_∞	Max Controlled k_∞
1	A9-458L-8G6	1.2420	1.0719
2	A9-458L-8G6-4G3	1.2408	1.0710
3	A9-390L-8G5	1.2366	1.0636
4	A9-396L-8G5	1.2365	1.0631
5	A9-434-10G6	1.2353	1.0636
6	A9-459L-12G7	1.2227	1.0541
7	A9-406-11G6	1.2189	1.0478
8	A9-430-11G7	1.2100	1.0411
9	A9-459L-12G8	1.2061	1.0390
10	A9-453-11G8	1.2036	1.0366
11	A9-456L-12G8	1.2011	1.0357
12	A9-456L-12G8-4G3	1.1980	1.0327
13	A9-396L-8G7-4G8	1.1959	1.0288
14	A9-403-13G7	1.1926	1.0257
15	A9-427-12G8	1.1883	1.0235
16	A9-421-13G8	1.1811	1.0173
17	A9-391L-12G8	1.1778	1.0151

Table RAI-28.4: Maximum in-Rack k_∞ For ATRIUM-9B Fuel

Lattice	in-rack k_∞
Bounding	0.8843
A9-458L-8G6	0.8841
A9-458L-8G6-4G3	0.8776
A9-390L-8G5	0.8766
A9-396L-8G5	0.8747
A9-434-10G6	0.8762
A9-459L-12G7	0.8697
A9-406-11G6	0.8629
A9-459L-12G8	0.8580
A9-430-11G7	0.8467

Table RAI-28.5: GE14 Lattice Screening based upon Cold In-Core Geometry

No.	Lattice	Top height	Max Uncontrolled k_∞	Max Controlled k_∞
1	GE146096-451-11G80-4G70	54	1.1963	1.0331
2	GE146813-435-6G70-9G60	84	1.1942	1.0282
3	GE146814-429-6G70-9G60	96	1.1927	1.0208
4	GE146098-446-10G80-4G70	96	1.1887	1.0194
5	GE146097-451-10G80-4G70	84	1.1885	1.0268
6	GE146118-451-12G80-4G70	54	1.1856	1.0211
7	GE146809-430-2G80-7G70-5G60	96	1.1852	1.0150
8	GE146808-437-2G80-7G70-5G60	84	1.1832	1.0209
9	GE146120-446-11G80-4G70	96	1.1780	1.0079
10	GE146119-451-11G80-4G70	84	1.1778	1.0145
11	GE146812-435-18G70	54	1.1725	1.0119
12	GE146807-437-6G80-10G70	54	1.1704	1.0095
13	GE146815-429-6G70-9G60	144	1.1949	1.0338
14	GE146099-446-10G80-4G70	144	1.1918	1.0331
15	GE146810-430-2G80-7G70-5G60	144	1.1881	1.0284
16	GE146121-446-11G80-4G70	144	1.1805	1.0215

Table RAI-28.6: Maximum in-Rack k_∞ For GE14 Fuel

Lattice[1]	in-rack k_∞
Bottom Zone	
Bounding	0.8843
GE146096-451-11G80-4G70	0.8423
GE146813-435-6G70-9G60	0.8407
GE146118-451-12G80-4G70	0.8351
GE146097-451-10G80-4G70	0.8344
GE146808-437-2G80-7G70-5G60	0.8335
GE146119-451-11G80-4G70	0.8281
GE146814-429-6G70-9G60	0.8244
Top and Intermediate Zones	
Bounding	0.8869
GE146815-429-6G70-9G60	0.8487
GE146810-430-2G80-7G70-5G60	0.8438
GE146099-446-10G80-4G70	0.8437
GE146121-446-11G80-4G70	0.8383

[1] Due to the similarities between lattices 4 & 5, 7 & 8, and 9 & 10 of Table RAI-28.5, in-rack calculations were performed only for the higher enrichments variation of each pair.

Table RAI-28.7: ATRIUM-10 Lattice Screening based upon Cold In-Core Geometry

No.	Lattice	Max Uncontrolled k_∞	Max Controlled k_∞
Bottom Zone			
1	A10B-4399L-12G65	1.2262	1.0583
2	A10B-4537L-13GV70	1.2116	1.0482
3	A10B-4510L-13G75	1.2132	1.0461
4	A10B-4326L-15G65	1.2103	1.0442
5	A10B-4481L-12GV80	1.2085	1.0427
6	A10B-4253L-15G65	1.2078	1.0426
7	A10B-4459L-12GV80	1.2083	1.0426
8	A10B-4459L-13GV80	1.2072	1.0413
9	A10B-4511L-13G80	1.2058	1.0407
10	A10B-4502L-13G80	1.2055	1.0404
11	A10B-4466L-12G80	1.2027	1.0384
12	A10B-4507L-15G75	1.2015	1.0380
13	A10B-4504L-15G75	1.2015	1.0379
14	A10B-4538L-13GV80	1.1936	1.0322
15	A10B-4504L-16G75	1.1939	1.0319
16	A10B-4503L-15G80	1.1942	1.0314
17	A10B-4494L-15G80	1.1937	1.0311
18	A10B-4454L-14G80	1.1906	1.0271
19	A10B-4511L-16GV80	1.1828	1.0219
20	A10B-3993L-12GV80	1.1804	1.0194
21	A10B-3984L-12GV80	1.1802	1.0189
22	A10B-3726L-12G80	1.1676	1.0061
23	A10B-3618L-12G80	1.1663	1.0054
24	A10B-4023L-15GV80	1.1648	1.0053
Intermediate Zone			
25	A10T-4313L-15G65	1.2147	1.0482
26	A10T-4524L-13GV70	1.2144	1.0495
27	A10T-4451L-11G80	1.2138	1.0491
28	A10T-4455L-11G80	1.2131	1.0487
29	A10T-4229L-15G65	1.2117	1.0453
30	A10T-4307L-15G65	1.2108	1.0442
31	A10T-3987L-12G65	1.2099	1.0422
32	A10T-4431L-14G80	1.1871	1.0244
33	A10T-3947L-13GV70	1.1865	1.0255
34	A10T-3987L-12G80	1.1849	1.0205
35	A10T-4511L-15GV80	1.1836	1.0230
36	A10T-4042L-12GV80	1.1830	1.0218
37	A10T-4305L-16G75	1.1830	1.0215
38	A10T-4022L-12GV80	1.1823	1.0207

Table RAI-28.7: ATRIUM-10 Lattice Screening based upon Cold In-Core Geometry (continued)

No.	Lattice	Max Uncontrolled k_∞	Max Controlled k_∞
Top Zone[1]			
39	A10T-4444L-12G40	1.2764	1.1023
40	A10T-4400L-10G45	1.2751	1.1016
41	A10T-4409L-10G45	1.2745	1.1012
42	A10T-3986L-12G40	1.2570	1.0828
43	A10T-3947L-13GV38	1.2520	1.0800
44	A10T-4040L-10G45	1.2468	1.0763
45	A10T-4021L-10G45	1.2460	1.0751
46	A10T-4302L-13G65	1.2267	1.0569
47	A10T-4306L-16G65	1.2015	1.0367

[1] The Intermediate lattices also have a top lattice geometry and some of the lattices previously listed as intermediate extend into the Top Zone ("ABOVE 126"). The lattices listed in this section are generally more reactive due to the lower Gd content and only exist in the Top Elevation Zone.

2.23 *Request for Additional Information No. 32*

ANP-2843(P) (proprietary), Section 6.10 covers the interface between racks where inserts are credited and racks where degraded Boraflex is credited. The text in this section commits to placement of inserts into the degraded Boraflex racks such that there will be an insert between adjacent assemblies in the new and old regions.

From a technical point of view, doing this makes sense. However, the original criticality analysis should be reviewed to determine whether or not the coexistence of another storage rack region creates any new normal or credible abnormal conditions.

Confirm that the original criticality analysis is not impacted by the proposed changes. If necessary, update the analysis and implement any resulting modified or new controls.

Response:

As discussed in the response to RAI-2, the Technical Specifications will be changed to impose the same limits on fuel lattice k_∞ in all regions of the spent fuel pool and this represents a conservative decrease in assembly reactivity for assemblies allowed under the existing Boraflex analysis. As discussed in RAI-1 the addition of an insert into the Boraflex region conservatively lowers the reactivity in that region. Therefore, there are no normal or credible abnormal conditions that can increase the neutron multiplication in the Boraflex region of the pool.

2.24 *Request for Additional Information No. 34*

ANP-2843(P) (proprietary), Table 6.3 covers fuel and storage rack manufacturing uncertainty analysis. The following observations are made concerning the uncertainty analysis:

a. *The Gd rod pellet density and tolerance should be evaluated.*
b. *The insert wing width and tolerance should be evaluated.*
c. *The fuel channel manufacturing tolerances should be evaluated.*
d. *Many of the uncertainties presented will vary as some other parameters vary. A more complete parametric study is needed to provide bounding uncertainty estimates. For example, the Δk for the rod pitch uncertainty will vary with the number of Gd rods, Gd content of the Gd rods, fuel initial enrichment, fuel burnup, axial zone, fuel depletion conditions, etc.*
e. *The second footnote under Table 6.3 states that the value is equally valid for a fuel density of 95.85 percent TD. Was this calculated, or is it just the author's opinion? What is the purpose of this statement? Is the 95.85 percent value the nominal density for the Gd rods? If so, the uncertainty for the Gd rod density also produces an additional uncertainty in the Gd content for the rod. Thus it is unlikely that the density uncertainty for non-Gd rods and Gd rods would be the same.*
f. *Where KENO is used to calculate Δk values, the associated Monte Carlo uncertainty should be included in the Δk value.*

Where appropriate, revise the uncertainty analysis to address these issues.

Response:

a. The Gd rod pellet density and tolerance should be evaluated.

Additional fuel density cases have been run using an assembly with 10 gadolinia rods. The larger response was observed for the case where the density of the gadolinia pellet was decreased. This case has been added to Table RAI-34.1.

b. The insert wing width and tolerance should be evaluated.

A minimum representation of the insert wing width has been used so no tolerance data is needed or provided. See the response to RAI-18 for additional discussion.

c. *The fuel channel manufacturing tolerances should be evaluated.*

The fuel channel tolerance is addressed in Table RAI-34.1.

d. *Many of the uncertainties presented will vary as some other parameters vary. A more complete parametric study is needed to provide bounding uncertainty estimates. For example, the Δk for the rod pitch uncertainty will vary with the number of Gd rods, Gd content of the Gd rods, fuel initial enrichment, fuel burnup, axial zone, fuel depletion conditions, etc.*

The manufacturing tolerance uncertainties do not attempt to define the maximum possible uncertainty under any condition; rather these are the uncertainties that apply to the maximum reactivity lattices (Reference bounding lattices and/or REBOL lattices) that support the $k_{95/95}$ calculation. This is an appropriate approach because as the number of Gd rods is increased, or the gadolinia concentration is increased, or U235 enrichment is reduced, the overall reactivity decreases to a larger extent than the corresponding increase in the reactivity associated with the uncertainty.

e. *The second footnote under Table 6.3 states that the value is equally valid for a fuel density of 95.85 percent TD. Was this calculated, or is it just the author's opinion? What is the purpose of this statement? Is the 95.85 percent value the nominal density for the Gd rods? If so, the uncertainty for the Gd rod density also produces an additional uncertainty in the Gd content for the rod. Thus it is unlikely that the density uncertainty for non-Gd rods and Gd rods would be the same.*

The 3 enriched pellet densities that have been used with ATRIUM-10 fuel are listed in the following table. The criticality evaluation used the maximum stack density condition; therefore this evaluation provides conservative results for the 95.85% TD scenario.

[ ]

The impact of density uncertainty on Gadolinia rods is addressed in RAI-34(a).

f. Where KENO is used to calculate Δk values, the associated Monte Carlo uncertainty should be included in the Δk value.

The manufacturing uncertainties have been recalculated with the Monte Carlo standard deviation uncertainty added to the tolerance uncertainty in Table RAI-34.1. The fuel density for Gad pellets and channel thickness tolerances have also been added as requested in items (a) and (c). The Δk and standard deviation (s) values are combined as directed in the variance equation listed in Section 4.1.5 of the reference identified below,

$$\Delta k^2 = (u^2/\delta x^2)((k - k_{ref})^2 \pm (s_{MC}^2 + s_{MC,ref}^2))$$

where:	(k-kref)	change in keff induced by change δx on parameter x
	u	standard uncertainty of parameter x
	δx	change in parameter x

For this application the manufacturing tolerance results have been evaluated using the upper and lower bounds of the full tolerance range; therefore, δx represents a range greater than 2u. Rather than define a single uncertainty interval for this calculation and then multiply it by 2 to reestablish a 95/95 bounding interval, $u^2/\delta x^2$ will be conservatively treated as unity in this calculation.

For this application, the Monte Carlo uncertainty values have been added to the limiting case and where $(k - k_{ref})$ is negative for both the upper and lower bounds of the tolerance interval, a zero value has been used (e.g. the pellet diameter and insert thickness cases). The adjusted Δk values are the square root of the variance for that particular case. The statistically combined result is the square root of the sum of the variance values. As shown in Table RAI-34.1 the 0.0105 value used to represent the uncertainty due to manufacturing tolerances (i.e. Table 6.3 of ANP-2843) is also supported by this revised calculation.

Reference: ICSBEP Guide to the Expression of Uncertainties, Revision 5, V. F. Dean, September 30, 2008. {Distributed with the International Handbook of Evaluated Criticality Safety Benchmark Experiments, Nuclear Energy Agency, NEA/NSC/DOC(95)03, Sept. 2009 Edition.}

Table RAI-34.1: Manufacturing Reactivity Uncertainties

[ ]

---

1 Not independent of the "all rods" density case but it is conservative to add it to the table.

2 This is an insignificant parameter; its effect was combined with the U235 enrichment result.

3 The gadolinia uncertainty Δk includes a CASMO-4 based 0.002 Δk adder which accounts for differences at peak reactivity conditions.

4 Calculations at this uncertainty level produce a negative Δk. The Δk is set to zero and the effect of s_{MC} is applied for this case.

5 This is the square root of the sum of the variance of the tolerance values.

2.25 *Request for Additional Information No. 35*

In Section 6 of ANP-2843(P) (proprietary), provide a table showing the details of how all biases and uncertainties are combined to demonstrate compliance with applicable k_{eff} limits.

Response:

Within ANP-2843(P), the uncertainties associated with CASMO-4 are addressed in Section 6.2, the uncertainties associated with manufacturing tolerances are addressed in Table 6.3 and RAI response 34f, and the final multiplication factor is addressed in Section 6.6. A general overview of ANP-2843(P) is provided in Figure RAI-35.1.

Figure RAI-35.1: Overview of the ANP-2843(P) Criticality Safety Analysis

2.26 *Request for Additional Information No. 36*

ANP-2843(P) (proprietary), Section 7 provides the analysis conclusions. An explicit conclusion addressing compliance with GDC-5 and GDC-62, and with 10 CFR 50.68(b) should be stated.

Response:

As requested by the RAI above, this response is specific to ANP-2843(P). RAI-7 provides more specific information in regard to compliance with GDC-5 and 10 CFR 50.68(b)(7) in regard to the current LaSalle plant licensing basis.

General Design Criteria 5 addresses the sharing of structures, systems and components important to safety specifically to ensure that the ability to perform their safety function is not significantly impaired. As noted in RAI-7, the existence of a transfer canal allows for the transfer of fuel bundles between the unit specific spent fuel pools (i.e. the only shared components). As noted in the response to RAI-2, the requested change to TS Section 4.3.1 is being made to support this type of transfer. The Technical Specifications change represents an increase in the conservatism for the current analyses since it represents a reduction in the allowable reactivity for an assembly for storage in the Unit 1 spent fuel pool and the Boraflex regions of the Unit 2 spent fuel pool. Consequently, the ability of the spent fuel pool racks to maintain subcriticality is not impaired and the intent of GDC 5 is met.

General Design Criteria 62 specifies that criticality of fuel in handling or storage will be prevented by physical systems or processes. The intent of this license amendment request is to support this criteria with a physical change that introduces neutron absorbing material to the Unit 2 Boraflex racks in order to compensate for loss of the original absorber material. The purpose of the analysis in ANP-2843(P) is to provide assurance that criticality with the new rack configuration will not occur and therefore the intent of GDC 62 is met.

10CFR50.68(b) specifies a number of requirements that must be complied with by the licensee in lieu of maintaining a monitoring system capable of detecting a criticality as described in 10CFR70.24. Each requirement is addressed below:

1) *Plant procedures shall prohibit the handling and storage at any one time of more fuel assemblies than have been determined to be safely subcritical under the most adverse moderation conditions feasible by unborated water.*

   ANP-2843(P) establishes the SFP storage requirements that are reflected in the license amendment request change to TS Section 4.3.1. Implementation of the approved TS change in plant procedures is not part of the ANP-2843(P) criticality safety analysis. Fuel handling is not addressed by ANP-2843(P).

2) *The estimated ratio of neutron production to neutron absorption and leakage (k-effective) of the fresh fuel in the fresh fuel storage racks shall be calculated assuming the racks are loaded with fuel of the maximum fuel assembly reactivity and flooded with unborated water and must not exceed 0.95, at a 95 percent probability, 95 percent confidence level. This evaluation need not be performed if administrative controls and/or design features prevent such flooding or if fresh fuel storage racks are not used.*

   This requirement does not apply to ANP-2843(P) since this is not a fresh fuel storage criticality analysis.

3) *If optimum moderation of fresh fuel in the fresh fuel storage racks occurs when the racks are assumed to be loaded with fuel of the maximum fuel assembly reactivity and filled with low-density hydrogenous fluid, the k-effective corresponding to this optimum moderation must not exceed 0.98, at a 95 percent probability, 95 percent confidence level. This evaluation need not be performed if administrative controls and/or design features prevent such moderation or if fresh fuel storage racks are not used.*

   This requirement does not apply to ANP-2843(P) since this is not a fresh fuel storage criticality analysis.

4) *If no credit for soluble boron is taken, the k-effective of the spent fuel storage racks loaded with fuel of the maximum fuel assembly reactivity must not exceed 0.95, at a 95 percent probability, 95 percent confidence level, if flooded with unborated water. If credit is taken for soluble boron, the k-effective of the spent fuel storage racks loaded with fuel of the maximum fuel assembly reactivity must not exceed 0.95, at a 95 percent probability, 95 percent confidence level, if flooded with borated water, and the k-effective must remain below 1.0 (subcritical), at a 95 percent probability, 95 percent confidence level, if flooded with unborated water.*

   ANP-2843(P) was performed specifically to show that this requirement has been met. The applicable requirement is a k_{eff} of 0.95 at a 95 percent probability at a 95 percent confidence level since LaSalle is a BWR site with unborated water in the SFP. The analysis shows that the calculated $k_{95/95}$ value meets this requirement.

5) *The quantity of SNM, other than nuclear fuel stored onsite, is less than the quantity necessary for a critical mass.*

   This requirement does not apply to ANP-2843(P) since this analysis only addresses nuclear fuel storage in the SFP.

6) *Radiation monitors are provided in storage and associated handling areas when fuel is present to detect excessive radiation levels and to initiate appropriate safety actions.*

   This requirement does not apply to ANP-2843(P) since this is a criticality analysis only.

7) *The maximum nominal U-235 enrichment of the fresh fuel assemblies is limited to five (5.0) percent by weight.*

   The ANP-2843(P) criticality safety analysis establishes maximum allowable enrichments below the regulatory requirement and therefore complies with the intent of this requirement.

8) *The FSAR is amended no later than the next update which § 50.71(e) of this part requires, indicating that the licensee has chosen to comply with § 50.68(b).*

   Compliance with this requirement is the responsibility of the licensee and is not part of the ANP-2843(P) criticality safety analysis.

ANP-2843(P) complies with the intent of all of the applicable sections of 10CFR50.68(b).

Based upon the discussion above, ANP-2843(P) complies with the intent of GDC-5, GDC-62, and 10CFR50.68(b).

2.27 *Request for Additional Information No. 37*

ANP-2843(P) (proprietary), Section 7, first sentence:

> *This analysis demonstrates that all fuel assemblies delivered to the LaSalle Station (both Units 1 and 2) as of July 2009 can be safely stored in the LaSalle Unit 2 spent fuel pool with NETCO-SNAP-IN inserts.*

Contrary to this conclusion, the analysis, including that provided in Appendix B, did not show that all fuel currently at LSCS is acceptable for storage in the modified fuel storage racks. Instead, the analysis provided guidelines that could be used to check the existing inventory.

If the applicant does intend for the screening to be accomplished through this report, the logic supporting that the REBOL lattice calculations bound all existing inventory needs to be clarified and strengthened. This should include a more thorough discussion of variations in fuel assembly designs utilized at either unit and of how reactor operations have varied since initial startup. Comparisons between the REBOL lattices and peak k_∞ values for Gd assemblies must include consideration of the uncertainties associated with fuel burnup to the peak reactivity point. The existing spent fuel inventory should be screened to identify any assemblies that are atypical (i.e. damaged or modified fuel assemblies, assemblies that experienced unusual reactor conditions for an extended period of time, etc.). Such assemblies may still be acceptable for storage, but may require individual analysis.

Revise the text in Section 7 to fully and clearly address screening of the fuel inventory at both LSCS Units 1 and 2. If the intent was to screen all current inventory using the analysis presented in this report, strengthen the analysis to better support this screening.

Response:

The basic process used in the ANP-2843(P) criticality analysis to show compliance with the 95/95 keff criteria is summarized in Figure RAI-35.1. The analysis begins at the bottom of this figure with the screening of all previously manufactured fuel in the LaSalle Unit 1 and Unit 2 spent fuel pools.

All previously manufactured fuel at the LaSalle Station (used in Unit 1 and Unit 2) was screened and additional detailed information with regard to the fuel screening is provided in the response to RAI-28. Tables B.2 through B.6 of ANP-2843(P) provide the results of this screening, specifically providing the in-rack results for the limiting lattices for each fuel product line. The

limiting lattice for each of three axial zones used in the KENO criticality model is provided in Table B.1 of ANP-2843(P) along with a corresponding reference bounding lattice. The reference bounding lattice is defined to bound the in-rack reactivity of the limiting as manufactured lattice for each of the three axial zones of the KENO model.

The actual criticality safety analysis is performed with KENO and is based upon the REBOL lattices. As shown in the previously mentioned Table B.1 and Figure RAI-35.1, the REBOL lattices are defined with a reactivity of at least 0.010 Δk higher than the corresponding reference bounding lattice. All future ATRIUM-10 designs must meet the reference bounding lattice definitions. The intent of the 0.010 Δk adder is to account for the uncertainties associated with fuel burnup to the peak reactivity point. The appropriateness of this approach is addressed in the responses to several RAIs within this report, including RAI-22 and RAI-41. The criticality safety limitations for ATRIUM-10 fuel shown in Table 2.1 of ANP-2843(P) are for application to future ATRIUM-10 fuel to be used at LaSalle. As indicated in this response and RAI-28, all previously existing fuel of any design at LaSalle has been shown to be less reactive than the reference bounding design used in the ANP-2843 criticality analysis, and as such, meets the 95/95 keff criticality safety requirement.

The LaSalle units began operation in the early 1980s with an initial rated power of 3323 MWt. The initial cycles were considered 12 month cycles. Power uprates to 3489 MWt were implemented in both units during their respective Cycle 9. The cycle lengths transitioned from 12 to 18 to the current 24 month cycle length. As the cycle lengths increased, the fuel enrichment and gadolinia concentration has increased. The fuel product lines have been consistent between Units 1 and 2 and have been manufactured by either GNF (GE) or AREVA (SIEMENS, FRAMATOME). Table RAI-37.1 identifies the reload product lines by cycle for each unit.

During the operation history of the LaSalle units, fuel assembly failures have occurred and control rods have been inserted near the failed assemblies to suppress power in the failed assembly. This can lead to an extended period of depletion in a controlled state at a reduced power. The effect of depletion in a controlled state reduces the assembly reactivity relative to depletion in an uncontrolled state. Table RAI-37.2 provides comparisons of the peak in-rack k_∞ for both controlled and uncontrolled depletion at power densities of 50% and 100% of rated

power. The data provided in Table RAI-37.2 shows that controlled depletion reduces the maximum lattice reactivity compared to uncontrolled depletion. Operation for prolonged time periods with power suppression rods results in a decrease in reactivity relative to the lattice reactivity that has been used for the screening. Therefore operation with periods of extended control is conservative with respect to the criticality analysis.

Over the operating history of the two units, 32 assemblies have been identified to have experienced fuel failures or have had rods replaced prior to initial operation. These assemblies and the failure/modification state are identified in Table RAI-37.3.

With the exception of one assembly, the failed rods remain in the assembly or have been replaced with an inert rod. Insertion of an inert rod displaces fuel and does not increase the amount of moderation. Therefore, insertion of inert rods is conservative for the criticality evaluation.

Assembly 19A113 is missing the top 40" of a fuel rod. The removal of a fuel rod can increase the lattice reactivity. It is noted that for the same enrichment between an ATRIUM-10 bottom lattice and an ATRIUM-10 top lattice the increase in reactivity is approximately 0.003 Δk (in both KENO and CASMO) for the addition of 8 part length rods in an infinite array of lattices. This increase in reactivity is a result of an increase in the moderation within the fuel pin array. The removal of a single rod from a single assembly would have much less of a reactivity change than 8 rods in an infinite array of assemblies (i.e. the use of part length rods removes 8 rods from the top portion of the assembly). The actual rod that is severed is identified as F3 which is located adjacent to the ATRIUM-9 water channel. The maximum in-rack reactivity of the top lattice (A9-390-8G5) is 0.877 which is less than the reactivity of both the top and intermediate bounding lattices. Therefore the removal of the top portion of rod F3 does not result in a more reactive assembly than has been analyzed.

Table RAI-37.1: LaSalle Fuel Product Lines Used

Cycle	Unit 1	Unit 2
1	GE6	GE6
2	GE7	GE7
3	GE8	GE8
4	GE9	GE9
5	GE9	GE9
6	GE9	GE9
7	GE9	GE9
8	GE9	ATRIUM-9
9	ATRIUM-9	ATRIUM-9
10	ATRIUM-10	ATRIUM-10
11	GE-14	GE14
12	ATRIUM-10	ATRIUM-10
13	ATRIUM-10	ATRIUM-10 [1]
14	ATRIUM-10	(future cycle)

Note: GE6, GE7, GE8, and GE9 are all 8x8 designs. ATRIUM-9 is a 9x9 design. ATRIUM-10 and GE14 are 10x10 designs.

Table RAI-37.2: Uncontrolled and Controlled Depletion

	Uncontrolled Depletion k-infinity (in-rack)		Controlled Depletion k-infinity (in-rack)	
	100% PD	50% PD	100% PD	50% PD
Bottom				
A10B-4399L-12G65	0.871	0.872	0.867	0.868
A10B-4510L-13G75	0.863	0.865	0.849	0.850
A10B-4537L-13GV70	0.857	0.859	0.850	0.851
A10B-4538L-13GV80	0.844	0.846	0.840	0.841
Intermediate				
A10T-4313L-15G65	0.860	0.862	0.830	0.831
A10T-4524L-13GV70	0.860	0.861	0.843	0.844
A10T-4511L-15GV80	0.840	0.841	0.817	0.818
Top				
A10T-3947L-13GV38	0.882	0.884	0.861	0.862
A10T-4400L-10G45	0.907	0.908	0.895	0.896
A10T-4409L-10G45	0.907	0.908	0.895	0.896
A10T-4444L-12G40	0.907	0.909	0.899	0.900
ATRIUM-9				
A9-458L8G6	0.884	0.886	0.877	0.878

[1] Unit 2 Cycle 13 also includes eight (8) ATRIUM 10XM LTAs.

Table RAI-37.3: LaSalle Failed Fuel Assemblies

No.	Bundle	Damage/Modification
1	LJA202	Failed rod removed/Replacement rod inserted (bundle reconstituted prior to initial operation)
2	LJA023	Failed rod removed/Replacement rod inserted (bundle reconstituted prior to initial operation)
3	LJ9807	Failed rod removed/Replacement rod inserted (bundle reconstituted prior to initial operation)
4	LJ9577	Failed rod removed/Replacement rod inserted (bundle reconstituted prior to initial operation)
5	LYC390	Failed rod removed/Replacement rod inserted (bundle reconstituted prior to initial operation)
6	LYF373	Failed rod removed/Replacement rod inserted (bundle reconstituted prior to initial operation)
7	LYM142	Failed rod removed/Replacement rod inserted (bundle reconstituted prior to initial operation)
8	LYF289	Failed rods (2) removed after 1 cycle / Replacement rods (2) inserted for one additional cycle burn
9	30A042	Failed rod removed/Replacement rod inserted (Replacement rods inserted for one additional cycle burn)
10	40A096	Failed rod removed/Replacement rod inserted (bundle reconstituted prior to initial operation)
11	29A032	Failed rod and intact rod removed / Inert rods (2) inserted (original failed and intact rods shipped offsite for inspection)
12	29C170	Failed rod removed/Inert rod inserted
13	29C232	Failed rod removed/Inert rod inserted
14	28A034	Failed rod removed/Inert rod inserted
15	19A201	Failed rod removed/Inert rod inserted
16	19A077	Failed rod in bundle
17	19A113	Failed partial rod in bundle (top 40" in rod basket)

Table RAI-37.3: LaSalle Failed Fuel Assemblies (continued)

No.	Bundle	Damage/Modification
18	LJ9570	Failed rod in bundle
19	YJD643	Failed rod in bundle
20	YJD636	Failed rod in bundle
21	29C188	Failed rod in bundle
22	LYC294	Failed rod in bundle
23	29C220	Failed rod in bundle
24	19A080	Failed rod in bundle
25	30A061	Failed rod in bundle
26	YJ5835	Failed rod in bundle
27	30A270	Failed rod in bundle
28	JLR398	Failed rod in bundle
29	JLK143	Failed rod in bundle
30	JLK271	Failed rod in bundle
31	LJC175	Failed rod in bundle
32	33C308	Failed rod in bundle

2.28 *Request for Additional Information No. 38*

ANP-2843(P) (proprietary), Appendix A, page A-1, last paragraph - This paragraph provides guidance for using a different version of CASMO-4. The text states that changes no larger than 0.005 Δk are acceptable. There are two problems with this. First, use of an unvalidated computer code or nuclear data set for safety calculations is not acceptable. Second, if future 0.005 Δk differences were acceptable, the $k_{95/95}$ should be adjusted to include allowance for this rather large variation in CASMO-4 results.

The guidance giving permission to use a different version of CASMO-4 for acceptance screening should be removed.

Response:

This paragraph will be removed from ANP-2843(P). Any k_∞ comparisons will be performed with CASMO-4 as described in EMF-2158(P)(A) (Reference 12 of ANP-2843) which was the version used in ANP-2843(P).

2.29 *Request for Additional Information No. 39*

ANP-2843(P) (proprietary), Appendix C - The set of critical experiments used to validate the KENO calculations included 11 mixed uranium/plutonium-oxide (MOX) configurations. The average keff values for the non-MOX and MOX configurations are 0.9942 and 0.9998, respectively. Considering that all of the KENO calculations used in the criticality analysis were for fresh fuel that did not include plutonium, inclusion of the MOX critical experiment results is not appropriate. Even if they were retained, trending analysis as a function of plutonium (Pu) content would reveal a statistically significant trend would need to be factored into calculation of bias and bias uncertainty.

For validation of fresh fuel calculations, remove the MOX experiments from the validation set and recalculate the bias and bias uncertainty.

If the analysis is expanded such that validation of burned fuel calculations is needed, include the mixed-oxide critical experiments documented in NUREG/CR-6979, "Evaluation of the French Haut Taux de Combustion (HTC) Critical Experiment Data" (ADAMS Accession No. ML082880452), in the burned fuel validation set.

Response:

The set of 100 critical KENO benchmarks is a standard set forming the licensing basis that AREVA uses for spent fuel pool criticality analyses; they have been submitted, reviewed, and accepted for several previous criticality analysis submittals for other licensees. Benchmark results obtained for the MOX criticals compare well with the experimental results and demonstrate the validity of the methodology for modeling a mixture of uranium and plutonium isotopes in fuel lattice geometries. Some previous submittals have included burned fuel models in the criticality analysis in order to provide a licensing basis for burnup credit in the spent fuel pool. Recently, the NRC has requested that the NUREG/CR-6979 MOX benchmarks be added to the licensing basis for a submittal that includes burnup credit, and both AREVA and the licensee have agreed to comply.[1] For a submittal where only fresh fuel calculations are being performed with KENO V.a (i.e. as in ANP-2843(P)), AREVA intends to maintain this set of 100 benchmark cases, including the 11 MOX criticals. The benchmarks are used to test the overall adequacy of the KENO V.a approximations of the solution and library used for LWR storage of fuel. The rationale has been that the validation set represents possible materials and

[1] However, for the Exelon submittal containing ANP-2843(P), compliance with the 95/95 Keff criticality analysis does not rely on fuel storage within any assumed burnup band, i.e. the ANP-2843(P) criticality analysis does not credit fuel burnup in the licensing basis.

configurations for LWR fuel storage and this set has been reviewed and approved. It was not intended to be custom fitted to each application.

This approach of including the MOX criticals in the ANP-2843(P) analysis is questioned in the RAI above. To demonstrate that this approach remains reasonable, a trending comparison with Pu content is shown in Figure RAI-39.1. This figure demonstrates that the current application of the 95/95 lower tolerance limit for a normal distribution (K_L) is more limiting at 0 wt% Pu than the lower tolerance band that accounts for the trend line. In addition, Table RAI-39.1 shows a comparison of parameters for the full set of 100 benchmarks versus the reduced set of 89, which excludes the MOX criticals. The bias and bias uncertainty results do not change significantly and the 95/95 lower tolerance limit for a normal distribution (K_L) values are identical to 4 significant digits. Therefore, this set of 100 cases remains applicable for the method uncertainty determination.

Table RAI-39.1: Comparison of Parameters for Datasets with and without MOX

Parameter	UO_2 + MOX, n = 100	UO_2 only, n = 89
Weighted Average k_{eff}	0.99458	0.99448
k_{eff} Bias	-0.00542	-0.00552
S_P	0.00511	0.00505
$C_{95/95}$	1.927	1.946
Bias Uncertainty	0.00985	0.00983
K_L	0.98472	0.98465

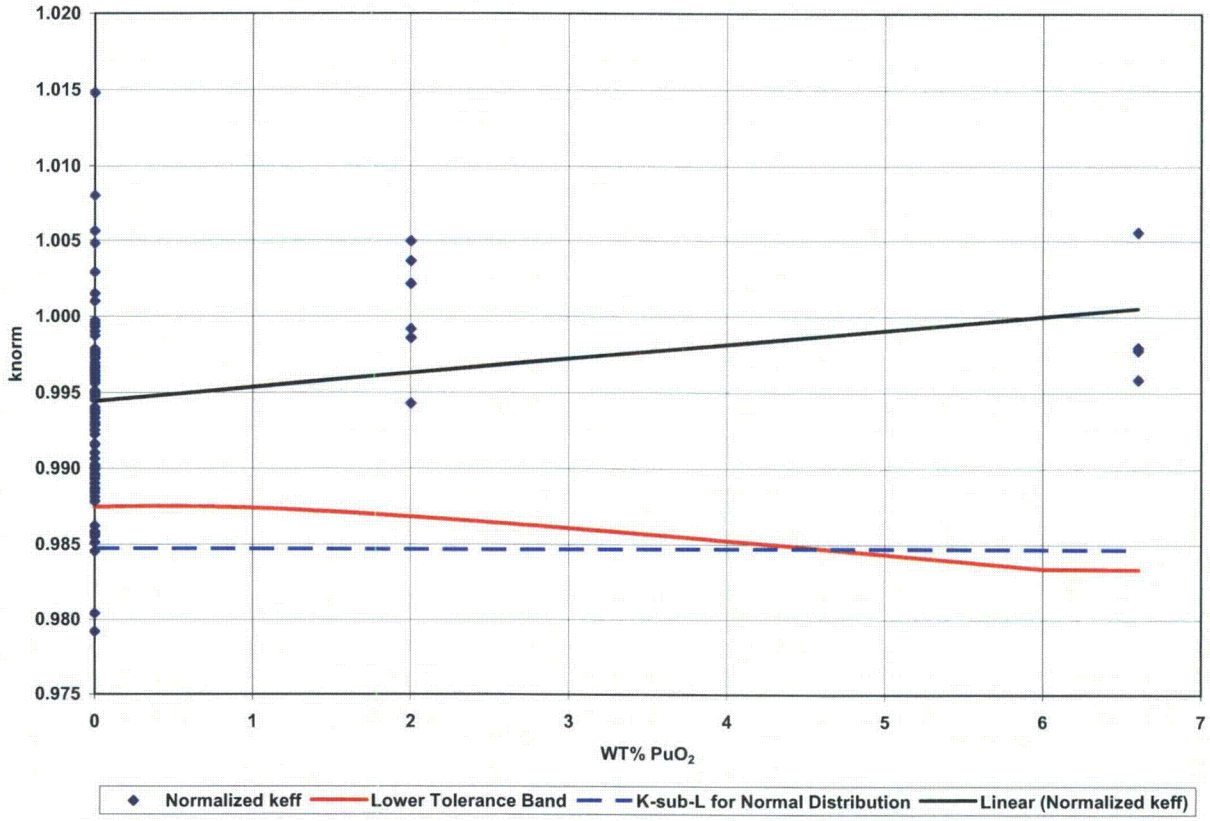

Figure RAI-39.1: Evaluation for Pu Trend

2.30 *Request for Additional Information No. 40*

Describe the statistical method and acceptance/rejection criteria used for determining that there are no trends in the data in Table C.5 in ANP-2843(P) (proprietary). Provide a reference describing the statistical method. While the ITI>t and the p-values are low for EALF and enrichment trends, it is not clear that no valid trends exist.

Response:

The statistical method is based on the calculated coefficient of determination (r^2), the calculated T-statistic (T), the associated probability (P-value, probability of $T_{(n-2)} > T_{Calculated}$), and the appearance and distribution of the plotted standardized residuals. This methodology is aptly described in Section C.5 with citations to source references where deemed necessary. However, several minor errors were noted and the text of Section C.5 and several Table C.5 entries were corrected (see below). Statistical evidence for the existence of trends for EALF and enrichment include T-values that exceed the critical value of the t-distribution (2-sided, α = 0.05/2) with corresponding probabilities that are less than 10% (P-value < 0.10). Linear regression and correlation is discussed in Chapter 10 of Reference C.7, particularly Sections 10.3 and 10.4 (pp. 366 – 391). Evidence against the existence of statistically significant trends are $r^2 << 1.0$, P-value > 0.01, and the skewed shape of the plot of standardized residuals, which are not distributed normally about a mean value of zero.

Reference C.8 recommends the use of the Anderson-Darling test to verify a data sample is distributed normally (see pp. 372 – 373 of Reference C.8). Anderson-Darling test results obtained for the standardized residuals of the EALF and enrichment trends were A* = 1.28 and A* = 1.15, respectively; both results exceed the critical value (A* = 0.752) for a significance level of 5% (α = 0.05), thus the null hypothesis of normality is rejected. While the evidence must be weighed subjectively, AREVA's conclusion is that there are no statistically significant or valid trends affecting the criticality bias evaluation. This same conclusion is documented in several previously approved licensing submittals. However, if the evidence of trends for EALF and enrichment were accepted, lower tolerance bands could be calculated, which would appear as shown in the following figures. In comparison to the K_L = 0.9847 limit that was determined based on a normal distribution of data with no significant trends (see RAI-39), the lower tolerance limit is conservatively bounding for all but the highest end of the ranges. At the high

end of the range, the non-conservatism is acceptably small and results primarily from the sparseness of the data, in comparison to the lower end of the range.

References for the above responses (taken from ANP-2843(P)):

C.7 Rosencrantz, W.A., *Introduction to Probability and Statistics for Scientists and Engineers*, McGraw-Hill, New York, NY, 1997 (copyright year also needs to be corrected to 1997 in ANP-2843(P)).

C.8 D'Augustino, R.B. and Stephens, M.A, *Goodness-of-Fit Techniques*, Statistics Textbooks and Monographs, Volume 68, New York, NY, 1986.

Minor Corrections Required for the Text of ANP-2843(P)

Section C-5, page C-12: the formula for 's' should be 's^2', as shown below:

$$s^2 = \frac{1}{n-2}\sum_{i=1,n}(y - \hat{y}_i)^2$$

Also, in the following paragraph:

The test statistic is compared to the Student t-distribution ($t\alpha/2,n-2$) with 95% confidence and n-2 degrees of freedom (Reference C.8, p.T-5), where n is the initial number of points in the subset.

Given a null hypothesis $H0:\beta1=0$, of "no statistically significant trend exists (slope is zero)", the hypothesis would be rejected if $|T| > t\alpha/2,n-2$. By only accepting linear trends that the data supports with 95% confidence, trends due to the randomness of the data are eliminated. A good indicator of this statistical process is evaluation of the P-value probability that gives a direct estimation of the probability of having linear trending due only to chance.

The citation to Reference C.8, p. T-5 should be for:

Natrella, M.G. 1963, *Experimental Statistics*, National Bureau of Standards Handbook 91, Washington DC, US Department of Commerce, National Bureau of Standards.

The citation could also be changed to Reference C.7, p. 371, which is also applicable and adequate.

Section C-5, page C-13: top of page, paragraph ending as follows:

These requirements were verified for the present calculation by applying an omnibus normality test (Reference C.8, p.372) on the residuals.

The parentheses should also show 'Anderson-Darling', as in: '(Anderson-Darling, Reference C.8, p. 372)'.

Also, Table C.5: the $t_{0.025,n-2}$ values should be 2.276 (not 1.987) for EALF, H/X, and Boron trends, and 2.281 (not 1.991) for the enrichment trend. In addition, the n value for the enrichment trend should be 89 (not 90).

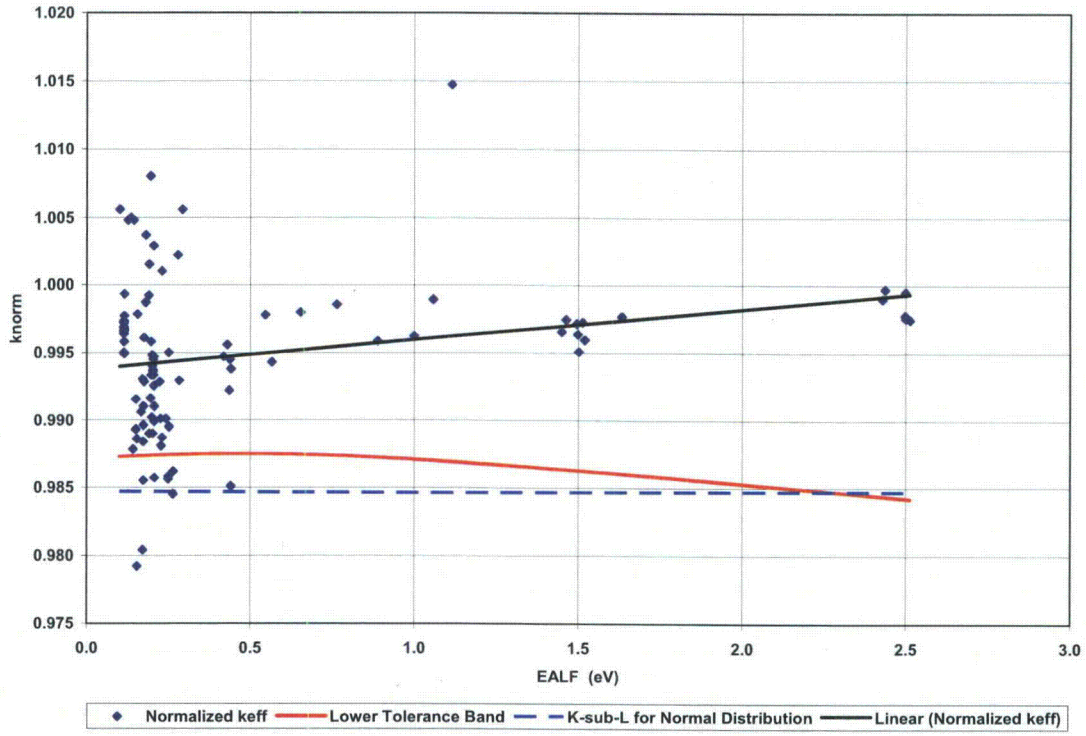

Figure RAI-40.1: Evaluation for EALF Trend

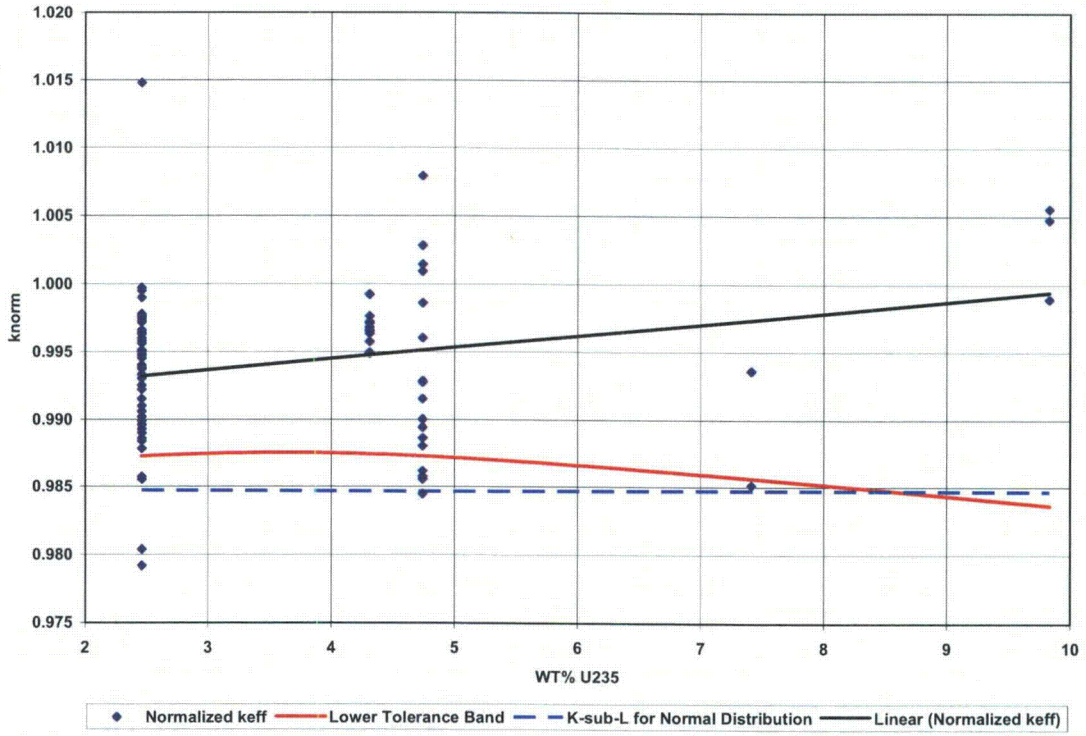

Figure RAI-40.2: Evaluation for Enrichment Trend

2.31 *Request for Additional Information No. 41*

ANP-2843(P) (proprietary), Appendix D, Section D.3.3 - This section provides a 0.0030 Δk depletion uncertainty and cites reference D.3 [EMF-2158(P)(A)]. The uncertainties presented in reference D.3 are for the combination of CASMO-4 and MICROBURN-B2. It is not clear that the CASMO-4+MICROBURN-B2 uncertainty applies to the in-rack storage calculations. In reactor geometry, offsetting errors associated with variation from fresh to high burnup fuel may mask a burnup-dependent trend. The reactor simulation uses many CASMO calculations, while the spent fuel storage racks peak reactivity calculation uses three, none of which are fresh fuel. The differences between the reactor simulation and the in-rack k_∞ calculations are so significant that little confidence can be placed in the CASMO-4 depletion uncertainty value adopted in Section D.3.3.

Provide better justification for the CASMO-4 depletion uncertainty used in the analysis.

Response:

The purpose of Appendix D is to provide a qualification basis for the use of CASMO-4 for the subset of calculations in which this code is used. This subset of calculations includes those that require a depletion component. Ultimately, the intent of Appendix D is to support 1) the translation of the REBOL lattices from CASMO-4 to KENO, and 2) the 0.010 Δk adder used in the definition of the REBOL lattices to account for CASMO-4 uncertainty. This RAI questions the validity of one of the components used to support the 0.010 Δk adder.

The approach taken in Section D.6 of ANP-2843(P) is to define an uncertainty term which can be subdivided into depletion and calculational uncertainty components. The calculational uncertainty was established by direct comparison to in-rack KENO calculations. This code-to-code comparison provides a link to the critical experiments through the ANP-2843(P) Appendix C benchmarking (i.e. KENO benchmark analyses to a series of critical experiments). This indirect comparison technique is required since CASMO-4 is an infinite lattice code and the benchmark experiments are composed of finite critical geometries. The adequacy of the calculation uncertainty component is addressed in more detail in the responses to RAI-42 and RAI-43.

The separate depletion component that is the subject of this RAI is necessary since the KENO code does not include depletion capability and depletion is not addressed by the set of critical experiments provided in Appendix C. The use of the [ ]

[

]

One of the concerns stated in the RAI above is that reliance upon [ ] may in fact mask burnup dependent trends due to the mixture of fresh and exposed fuel. EMF-2158(P)(A) also reports [

]

In the ANP-2843(P) analysis, the CASMO-4 depletion uncertainty is only used to justify the 0.010 Δk adder. The calculated value in Appendix D of the combined CASMO-4 uncertainty including the estimated depletion uncertainty is [ ] to the 0.010 Δk adder that was actually used. This margin allows for a significant increase in the assumed CASMO-4 depletion uncertainty without invalidating the basis of the criticality analysis.

The response to RAI-22 provides a separate justification based upon an alternate Kopp approach which results in a maximum depletion and residual gadolinia uncertainty of 0.0078 Δk for the reference bounding lattices. This method double counts the residual gadolinia impact as illustrated in Figure RAI-22.1 and still supports the 0.010 Δk adder with a 2.2 mk margin.

2.32 *Request for Additional Information No. 42*

ANP-2843(P) (proprietary), Appendix D, Section D.5.1, "Area of Applicability" - The AOA should be more fully described. The CASMO-to-KENO comparisons were performed with only fresh Atrium 9 and 10 fuel having enrichments ranging from 2.2 to 3.1 wt percent ^{235}U, in assemblies that had no Gd rods, and at temperatures of 4, 20, and 100 degrees Celcius.

Revise the AOA to more accurately describe the range of the code-to-code comparisons that are made. Justify the extension of the AOA beyond the parameters evaluated.

Response:

The statement provided in Section D.5.1 "Area of Applicability" is as follows:

> *The fuel and rack geometry as well as fuel enrichment were evaluated consistent with the LaSalle Unit 2 spent fuel pool. Therefore the area of applicability is specific to the LaSalle Unit 2 spent fuel pool with inserts.*

The primary intent of this statement is to limit applicability of the code-to-code comparisons to the analysis in ANP-2843(P) since the configuration and analysis conditions are specific to the LaSalle Unit 2 SFP with inserts. [

] which were defined to be 0.010 Δk more reactive than the reference bounding lattices. The in-rack calculations include the geometry and materials consistent with the Unit 2 Rack design with inserts and no credit for Boraflex, the same model used in the main criticality evaluation. The temperatures bound the limiting cases for the criticality evaluation.

As discussed in the response to RAI-23, [

]. Consequently, the statement in D.5.1 AOA accurately reflects the analysis performed.

2.33 *Request for Additional Information No. 43*

ANP-2843(P) (proprietary), Appendix D, Section D.5.2 - Note that variations in initial enrichment were studied and for only Atrium 9 and 10 assembly designs. Code-to-code variations in Δk due to variations in densities, wall thicknesses, pin pitches, Gd concentrations, areal ^{10}B densities, etc. were not studied.

Expand the analysis presented in D.5.2 to provide bias and bias uncertainty estimates for using CASMO-4 to calculate the uncertainty quantities used in Section 6.

Revise the AOA to more accurately describe the range of the code-to-code comparisons for calculation of Δk values. Justify the extension of the AOA beyond the parameters and fuel assembly designs evaluated.

Response:

As discussed in the response to RAI-42, [

]

Referring to Figure RAI-35.1, CASMO-4 is used to define a set of reference bounding lattices that are more reactive than all past and allowed future fuel lattices. The manufacturing tolerance uncertainties are calculated with KENO and not CASMO-4[1]. At no time will CASMO-4 results be used to calculate a $k_{95/95}$ value; therefore, it is not necessary to quantify the manufacturing uncertainties for use with CASMO-4 as was done for KENO V.a in Table 6.3 of ANP-2843(P) as supplemented by the response to RAI-34. In this evaluation, CASMO-4 is used to identify the most reactive previously manufactured lattices, define reference bounding lattices, and define REBOL lattices for use in KENO V.a. KENO is then used to perform the calculations needed to support the $k_{95/95}$ calculation.

The application of the KENO V.a to CASMO-4 comparisons performed in Section D.5.2 of ANP-2843(P) is discussed in more detail in the response to RAI-45. The purpose of the code-to-code comparisons in Appendix D of ANP-2843(P) is discussed in the response to RAI-23.

[1] The one exception is the calculation of a depletion adder (0.002) to the Gadolinia concentration uncertainty, as identified in the footnote to Table 6.3 of ANP-2843(P).

2.34 *Request for Additional Information No. 44*

ANP-2843(P) (proprietary), Appendix D, Section D.6, footnote at the bottom of page D-17 - From the discussion provided in the footnote, there appears to be some confusion concerning the "5% of the reactivity decrement" uncertainty suggested by Kopp in Reference D.1. This uncertainty was intended to cover uncertainty in the calculation of burned fuel compositions and in calculating keff for systems with burned fuel. The reactivity decrement uncertainty was not meant to cover modeling simplifications and approximations.

The peak reactivity for a BWR Gd assembly includes credit for both fuel burnup and for residual Gd. As applied to BWR fuel assemblies with Gd rods, the uncertainties due to changes in actinide and fission product compositions should be calculated separately from the uncertainty due to modeling of Gd depletion.

The suggested 5 percent of the reactivity decrement applies only to the reactivity decrement associated with changes in actinides and fission products. It is necessary to also adopt some additional uncertainty associated with calculation of the amount of gadolinium still present at peak reactivity.

While it is not clear, the analysis presented in the footnote appears to be taking 5 percent of the reactivity increase from zero burnup to the peak burnup point. This is not consistent with the uncertainty suggested by Kopp in Reference D.1.

Revise or remove the discussion provided in the footnote.

Response:

The original approach suggested by Kopp in Reference D.1 of ANP-2843(P) was to quantify a depletion uncertainty for burnup credit analyses (i.e. analyses that credit the reactivity reduction due to fuel burnup past peak reactivity conditions). The LaSalle Unit 2 SFP criticality analysis provided in ANP-2843(P) is not a burnup credit analysis but instead is performed assuming all fuel is at the peak reactivity condition (i.e. compliance with the 95/95 Keff criticality analysis does not rely on fuel storage within any assumed burnup band). The purpose of the footnote is to provide additional justification for the treatment of the CASMO-4 0.010 Δk adder used in the definition of the REBOL lattices.

The response to RAI-22 provides an alternate evaluation based upon the discussion provided in the RAI above.

2.35 *Request for Additional Information No. 45*

ANP-2843(P) (proprietary), Appendix D, Section D.7, First paragraph - The conclusion stated in the 1st paragraph is overly broad. The AOA for the analysis reported in Appendix D was much narrower than is suggested by the conclusion.

It is not clear exactly what the 3rd paragraph is trying to accomplish. However, there does not appear to be any analysis provided in Appendix D that evaluated lattice-specific bias dependence relative to use of CASMO-4 for the various lattices. Provide the logic supporting this assertion or remove this text.

Fourth paragraph - It is not clear that the 0.01 Δk adder is adequate to cover uncertainties associated with calculation of peak rack k_∞ values.

Revise the conclusions to more clearly and accurately state the conclusions that can be drawn from the work presented in Appendix D.

Also, explain how the CASMO bias and bias uncertainty determined in Appendix D are incorporated into the maximum k_{eff} determination.

Response:

The basic conclusion of the first paragraph in Section D.7 is:

> *... that the CASMO-4 code can be used for the characterization of in-rack reactivity of fuel designs in the LaSalle Unit 2 spent fuel pool.*

Based on EMF-2158(P)(A) and the comparisons provided in Appendix D of ANP-2843(P), the CASMO-4 code has been shown to be capable of characterizing the depletion and relative lattice reactivity of nuclear fuel. This is further supported by the responses to RAI-41, RAI-42, and RAI-43. Additional justification to support the estimated magnitude of calculational uncertainty is provided with an alternate calculational approach as discussed in the response to RAI-44 and developed in detail in the response to RAI-22.

The comparison with respect to the three geometries included in Table RAI-45.1 showed that both CASMO-4 and KENO V.a trended the reactivity consistently. This was not a quantitative statement with regard to the accuracy. The ATRIUM-9 and ATRIUM-10 geometries were chosen since they represent the limiting lattices in the Unit 2 SFP as discussed in the response to RAI-42. The lattice specific bias dependence is shown below for the 4 °C cases. [ ]

[

]

Table RAI-45.1: CASMO-4 to KENO Lattice Geometry Dependence at 4°C

[ ]

The purpose of the Appendix D comparisons and their application to $k_{95/95}$ are summarized below.

Section D.5.1 of ANP-2843(P) shows [

]

[1] The values for 'all lattices' are provided at 4°C which is the same basis as the individual lattice results. These values are different than those provided on page D-11 of ANP-2843(P) which is based upon all calculated temperatures.

[

]

Section D.6 of ANP-2843(P) evaluates the calculational and depletion uncertainties associated with CASMO-4. (This value is also supported by an alternate method in the response to RAI-22). Additional margin is conservatively included beyond the calculated uncertainties to define the 0.010 Δk adder that is used when defining the REBOL lattices.

The final $k_{95/95}$ value includes the CASMO-4 calculational and depletion uncertainties associated with the 0.010 Δk adder as a bias value imbedded in the 0.916 in-rack k_{eff} value. This is accomplished by increasing the U235 enrichment level of the REBOL lattices.

3. Follow-up Request for Additional Information

A follow-up request for additional information was provided to Exelon Nuclear as documented in Reference 4. The following provides the text of the request and AREVA's response.

Request for Additional Information (not numbered)

As described in Section 6.0, the primary fuel storage rack model appears to be three infinite slabs of the bottom, middle and top limiting assembly lattices, with a periodic boundary condition utilized below the bottom slab and above the top slab. The applicant should provide justification for use of this non-physical model of the spent fuel storage racks. The justification should address why this non-physical model is conservative compared to reality.

Response:

The KENO in-rack model as described in Section 6.3 of ANP-2843(P) includes periodic boundary conditions for all three dimensions, this includes the axial dimension. The use of a periodic boundary condition results in the model containing fissile material above and below the physical boundaries of the rack. As the reviewer states above, this is non-physical when compared to the actual rack geometry which actually consists of a water reflector above the rack and a combination of water, concrete, and other structural materials below the rack.

The use of infinite axial modeling of the fuel is supported by the Kopp letter (section 5.A.3.c of Reference D.1 of ANP-2843(P), shown below), which states:

c. *The spent fuel storage racks should be assumed to be infinite in the lateral dimension or to be surrounded by a water reflector and concrete or structural materials as appropriate to the design. The fuel may be assumed to be infinite in the axial dimension, or the effect of a reflector on the top and bottom of the fuel may be evaluated.*

The use of a multiplying medium (i.e. additional fissile material) in lieu of a reflector interface at the boundaries of the rack would be expected to provide a conservative k_{eff} calculation. To verify this assumption additional KENO in-rack calculations have been performed as detailed below:

Case 1: A water reflector is specified for the axial (z direction) boundary condition.

Case 2: A water reflector is specified for the top boundary condition. The bottom boundary is modeled with twelve (12) inches of water below the active fuel region with a twenty-four (24) inch concrete reflector.

Case 2 more closely models the actual geometry of the spent fuel pool, except that the stainless steel pool liner and other structural components have been conservatively neglected[1]. It is also noted that the dimensions were chosen to be representative for the purposes of this sensitivity analysis and were not chosen as an exact representation of the LaSalle spent fuel pool.

Table RAI-U.1 provides the comparison of the results for these cases. This comparison confirms that the axial periodic boundary condition used in the KENO calculations of ANP-2843(P) provides a significant degree of additional conservatism (> 0.009 Δk).

Table RAI-U.1: KENO Axial Boundary Condition Comparisons

	In-Rack k-eff	Axial Boundary Condition
Base Case	0.9152 [2]	Periodic (infinite axial fissile material)
Case 1	0.9047	Water Reflector (top and bottom)
Case 2	0.9054	12 inches of Water and 24 inch concrete reflector (bottom) – Water reflector (top)

1 The stainless steel material in the liner is the primary additional structural material that is not modeled. Other significant structural components not modeled include lower and upper tieplates on the fuel bundles and parts of the rack module outside of the active fuel zone. These structural components act as parasitic absorbers and not including them provides a more conservative calculation.

2 This value was rounded up to 0.916 in the $k_{95/95}$ calculation in Section 6.6 of ANP-2843(P).

4. References

1. USNRC Letter to Exelon Nuclear (Cameron S. Goodwin to Charles G. Pardee), LASALLE COUNTY STATION, UNITS 1 AND 2 – REQUEST FOR ADDITIONAL INFORMATION RELATED TO LICENSE AMENDMENT REQUEST REGARDING THE USE OF NEUTRON ABSORBING INSERTS IN UNIT 2 SPENT FUEL POOL STORAGE RACKS (TAC NOS. ME2376 AND ME2377), April 26, 2010.

2. Exelon Letter to USNRC, LaSalle County Station, Units 1 and 2 Facility Operating Licensing Nos. NPF-11 and NPF-18, NRC Docket Nos. 50-373 and 50-374", RS-09-133. October 5, 2009.

3. ANP-2843(P) Revision 1, LaSalle Unit 2 Nuclear Power Station Spent Fuel Storage Pool Criticality Safety Analysis with Neutron Absorbing Inserts and Without Boraflex, August 2009.

4. USNRC Email to Exelon Nuclear (Cameron Goodwin to Ken Nicely), "LaSalle NETCO Insert Question," dated June 2, 2010 (ADAMS Accession Number ML101540001).

ATTACHMENT 6

AREVA NP Inc. Affidavit for Withholding CASMO-4 Version 2.05.09 User's Manual

AFFIDAVIT

STATE OF WASHINGTON)
) ss.
COUNTY OF BENTON)

1. My name is Alan B. Meginnis. I am Manager, Product Licensing, for AREVA NP Inc. and as such I am authorized to execute this Affidavit.

2. I am familiar with the criteria applied by AREVA NP to determine whether certain AREVA NP information is proprietary. I am familiar with the policies established by AREVA NP to ensure the proper application of these criteria.

3. I am familiar with the AREVA NP information contained in the report EMF-CC-230 Revision 0, entitled, "CASMO-4 Version 2.05.09 User's Manual," dated December 2006 and referred to herein as "Document." Information contained in this Document has been classified by AREVA NP as proprietary in accordance with the policies established by AREVA NP for the control and protection of proprietary and confidential information.

4. This Document contains information of a proprietary and confidential nature and is of the type customarily held in confidence by AREVA NP and not made available to the public. Based on my experience, I am aware that other companies regard information of the kind contained in this Document as proprietary and confidential.

5. This Document has been made available to the U.S. Nuclear Regulatory Commission in confidence with the request that the information contained in this Document be withheld from public disclosure. The request for withholding of proprietary information is made in accordance with 10 CFR 2.390. The information for which withholding from disclosure is

requested qualifies under 10 CFR 2.390(a)(4) "Trade secrets and commercial or financial information."

6. The following criteria are customarily applied by AREVA NP to determine whether information should be classified as proprietary:

(a) The information reveals details of AREVA NP's research and development plans and programs or their results.

(b) Use of the information by a competitor would permit the competitor to significantly reduce its expenditures, in time or resources, to design, produce, or market a similar product or service.

(c) The information includes test data or analytical techniques concerning a process, methodology, or component, the application of which results in a competitive advantage for AREVA NP.

(d) The information reveals certain distinguishing aspects of a process, methodology, or component, the exclusive use of which provides a competitive advantage for AREVA NP in product optimization or marketability.

(e) The information is vital to a competitive advantage held by AREVA NP, would be helpful to competitors to AREVA NP, and would likely cause substantial harm to the competitive position of AREVA NP.

The information in the Document is considered proprietary for the reasons set forth in paragraphs 6(b), 6(d) and 6(e) above.

7. In accordance with AREVA NP's policies governing the protection and control of information, proprietary information contained in this Document have been made available, on a limited basis, to others outside AREVA NP only as required and under suitable agreement providing for nondisclosure and limited use of the information.

8. AREVA NP policy requires that proprietary information be kept in a secured file or area and distributed on a need-to-know basis.

9. The foregoing statements are true and correct to the best of my knowledge, information, and belief.

SUBSCRIBED before me this 8th

day of June, 2010.

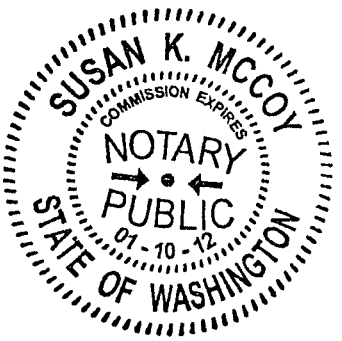

Susan K. McCoy
NOTARY PUBLIC, STATE OF WASHINGTON
MY COMMISSION EXPIRES: 1/10/12